Neural differentiation of human embryonic stem cells in a microfluidic system

Marc Isaksson

May 2015

LUNDS UNIVERSITET

Master's Thesis
Electrical Measurements

Faculty of Engineering, LTH
Department of Biomedical Engineering

Supervisor: Thomas Laurell

Acknowledgements

I would like to thank some people at the department of Biomedical Engineering in Lund. Many thanks to my supervisor professor Thomas Laurell for guiding me through this master thesis project and for providing me with hints regarding the design of a microfluidic gradient generator. Thanks to Axel Tojo for helping me to initiate this project. I would also like to thank researcher Martin Bengtsson for teaching me various fabrication processes in the clean room facility, and researcher Mikael Evander for tips regarding fabrication of PDMS injection molds.

At Wallenberg Neurocenter I would like to thank Dr. Agnete Kirkeby for initiating and managing the stem cell experiments. At last I would like to thank Associate Professor Malin Parmar for enabling the collaboration between Wallenberg Neurocenter and the department of Biomedical Engineering.

Abstract

The development of the human embryonic brain is a complex process involving several biological cues which interact to generate specific neural cells and anatomical features. There are still many questions to be addressed regarding biological key mechanisms which in case of malfunction might disturb the development of the brain. Animal models such as rats and mice have been used to get a better understanding of these biological mechanisms. However, it is essential to find a more suitable model system as the human brain is more complex and bigger in size.

The aim of this master thesis project is to create a microfluidic system capable of generating a model of the early developing brain from human embryonic stem cells.

Various microfabrication methods for creating the microfluidic system are presented along with simulations and fluorescence experiments. Also, stem cell differentiation experiments are performed and analyzed.

Results show that the microfluidic system can be used to create different cell types that constitute the early brain in a single cell culture. Simulations indicate that it is possible to test whether the design of the microfluidic system corresponds to the functional requirements.

A future optimized microfluidic system could enable the generation of more neural cell types and also recreate the anatomy of the early human brain.

Contents

1 Introduction

The human brain is a highly complex structure of the central nervous system (CNS). There is established knowledge about the physiology of the central nervous system but this knowledge is de facto very limited. Animal studies have so far provided superficial knowledge about functions of the human brain but many scientific questions remain to be addressed. How does neurodevelopmental disorders such as *attention deficit hyperactivity disorder* (ADHD), autism and dyslexia arise in some individuals? What are the reasons for developing neurological disorders such as Parkinsons, Alzheimer and Schizophrenia? One highly relevant question which remains to be answered is: How does the CNS develop in the human embryo and what could possibly perturbate this development? Developmental studies and toxicological studies have been performed using animal models but they entail several problems. A human brain is bigger and more complex than most commonly used research animals, as it is approximately 600 times bigger than the brain of a rat and 2000 times bigger than the brain of a mouse. Using animal models is also expensive as the estimated cost for testing one single substance for developmental neurotoxicity is $1.4 million [1]. In finding alternative approaches to animal testing in general, there have been research groups trying to create in vitro models which can mimic the function and the complexity of full-sized organs, so called Organs-On-Chips [2]. These chips are realized by combining tissue engineering with microfluidics and microfabrication. This project aims to create a developing-brain-on-a-chip, which is an organ-on-a-chip system mimicking the development of an early human brain structure known as the neural tube. Such a system would allow for genetic and dynamic studies where toxicological effects on the development of the neural tube can be evaluated. Such studies are otherwise not possible to perform due to the inability of using human embryos. A developing-brain-on-a-chip would also provide experimental evidence for the development of the human neural tube as there is no such model available today. The theoretical background will introduce the concepts of embryogenesis, microfluidics and microfabrication. It will be followed by the method treating simulations, fabrication processes and differentiation experiments that culminate in results and discussion.

2 Theoretical background

2.1 Development of the vertebrate central nervous system

2.1.1 Embryonic stem cells and the ectoderm

Embryonic stem cells (ESCs) are pluripotent meaning they have the ability to form any cell that constitutes the three germ layers in the gastrula during the vertebrate embryogenesis. It occurs during the process of gastrulation where ESCs in the blastula forms all of the three germ layers: endoderm, mesoderm and ectoderm, see figure 1. One part of the ectoderm differentiates into the neural plate comprising the origin of the central nervous system. [3] [4]

2.1.2 The neural tube

In a developmental event known as neurulation the late gastrula differentiates into the neurula. During this event the neural plate folds onto itself along the anteroposterior axis to form a hollow cylinder called the neural tube, see figure 2. [4]

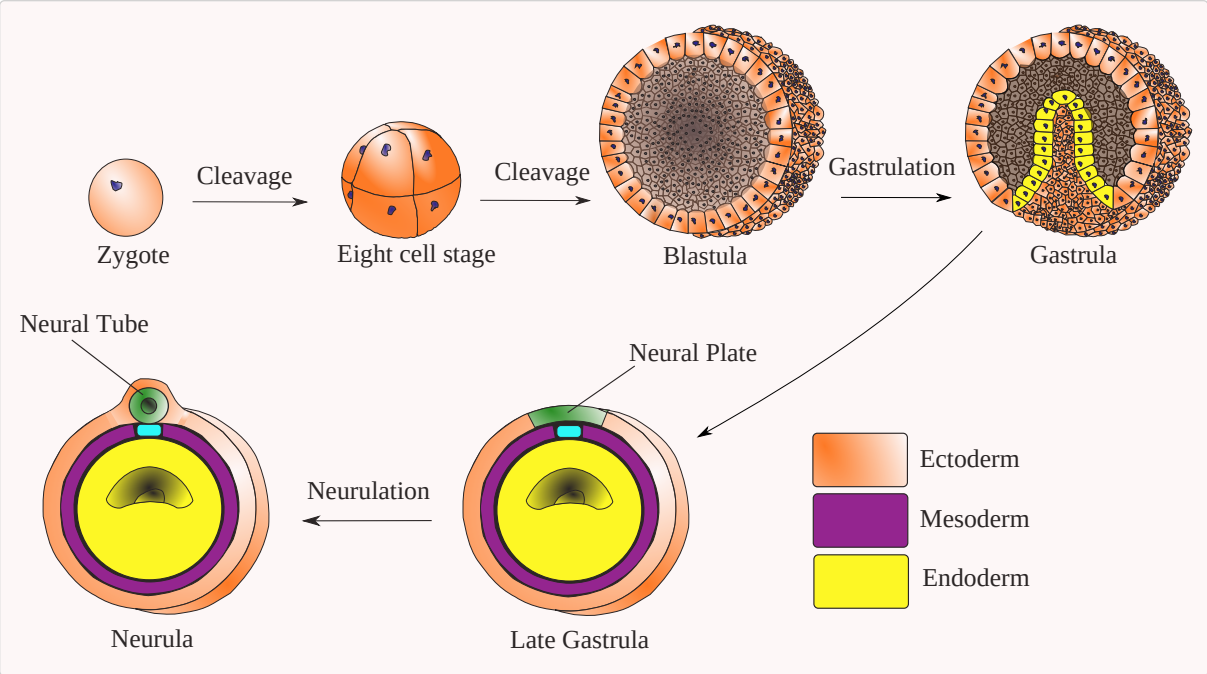

Figure 1: *Early development of the vertebrate embryo. A gastrula is formed through several cell cleavages and differentiating steps. In the late gastrula-phase, the neural plate is further developed into a neural tube in a process called neurulation. The three germ layers: ectoderm, mesoderm and endoderm are visualized with different colors.*

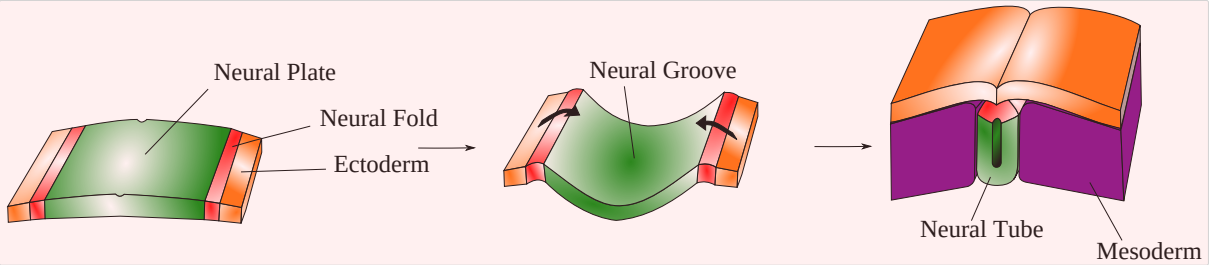

Figure 2: *Neurulation. As the neural plate begins to fold a neural groove appears. The neural tube is created upon completion of the folding process.*

Different cell types are generated in different areas of the neural tube as a result of two distinct signalling systems. The first signalling system patterns cells along the `rostro-caudal` (antero-posterior) axis while the second system patterns cells along the `dorso-ventral`(superior-inferior) axis, see figure 3a. Anterior(front) regions of the neural tube form the three cerebral vesicles called: *Prosencephalon*(forebrain), *Mesencephalon*(midbrain) and *Rhobencephalon*(hindbrain) while posterior (rear) regions form the spinal cord, see figure 3b. [5] [6]

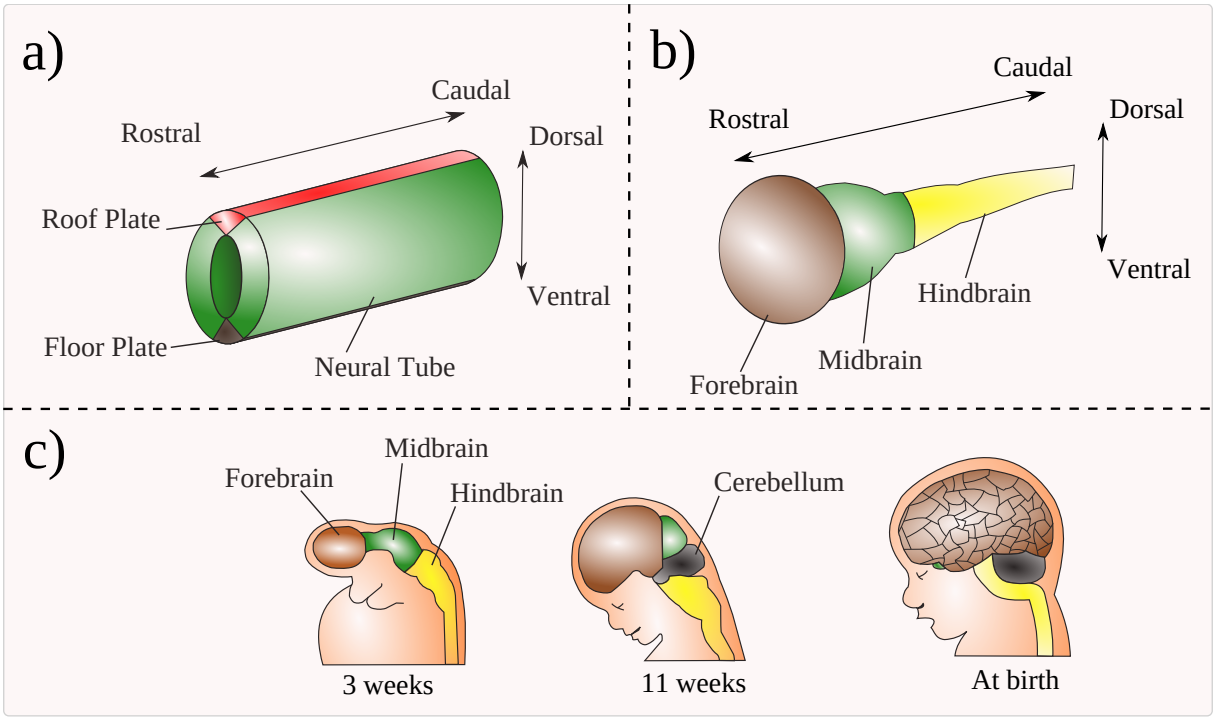

Figure 3: *a) Axes and orientations of the neural tube. b) Development of cerebral vesicles in the neural tube. c) Development of the central nervous system.*

2.1.3 Rostro-caudal patterning and morphogen gradients

In order to form all three cerebral vesicles there must be differentiation of cells having a rostral forebrain character into caudal neural cells constituting midbrain and hindbrain. This differentiating process is called rostro-caudal patterning and it is accomplished through the *canonical Wingless type-signalling pathway.* [7]. *Wingless type proteins*(WNTs) indirectly mediate developmental events during embryogenesis such as cell fate specification

and differentiation. These proteins act in a concentration-dependent manner to generate specific cell fates which is a characteristic of *morphogens*, see figure 4. Morphogens are defined as substances forming concentration gradients that act on cells to produce a specific response depending on the local concentration. [8] As WNT is expressed as a concentration gradient along the rostro-caudal axis of the neural tube, different cell types will be generated in the neural tube along this axis. The three cerebral vesicles are established as a result of this gradient. [6]

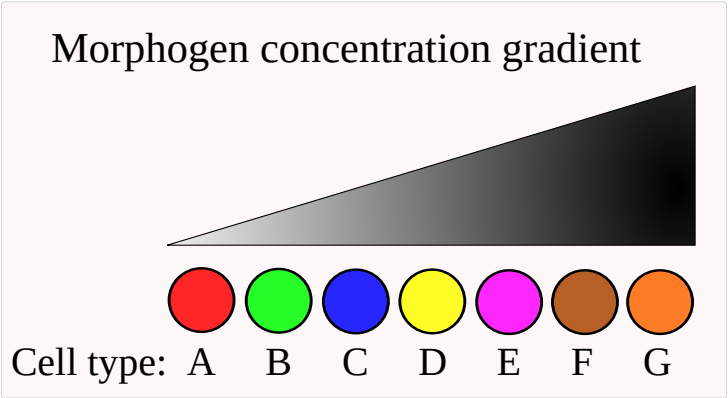

Figure 4: *Different cell fates are generated along the morphogen gradient.*

2.1.4 The role of Shh and BMP in dorso-ventral patterning of the neural tube

Additional signalling is required to generate neural diversity within each of the three cerebral vesicles. From the ventral floor plate of the neural tube emanate signal proteins called *Sonic hedgehog* (Shh) essential for cell patterning along the the dorso-ventral axis, see figure 5. Shh characterizes cell types lining the ventral half of the neural tube by acting as morphogen similar to WNT. [9] *Bone morpogenetic proteins* (BMPs) emanate

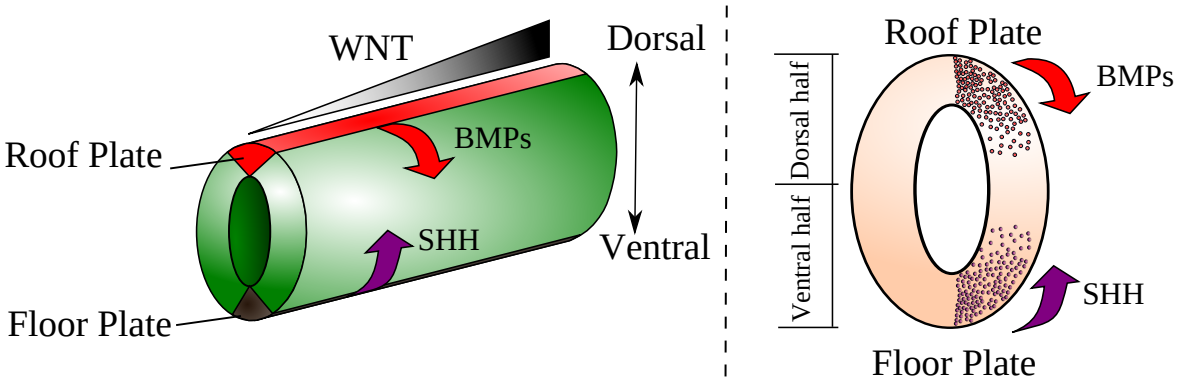

Figure 5: *Shh and BMP are emitted from the floor plate and the roof plate respectively to form morphogen gradients patterning cells along the dorso-ventral axis. The rostro-caudal patterning is also included to illustrate how the three different morphogens interact to pattern the neural tube, as seen by the WNT gradient.*

from the roof plate of the neural tube to pattern cells mainly on the dorsal half of the neural tube. [10]

2.2 Microfluidics

2.2.1 Short introduction to microfluidics

The physical behavior of many fluids are predictable and understood since we experience them in our everyday life. When adding milk to coffee it takes little effort to mix them evenly with a teaspoon. If the coffee would be substituted with honey it would however demand increased efforts in order to mix them thoroughly. A physical explanation for this observation is based on the fluids different viscosities. Water is a low viscosity fluid while honey is a high viscosity fluid resulting in the different behaviors. As the world is naturally percieved from a macroscopic point of view it may be believed that the behavior of fluids is independent of the geometrical dimensions confining them. But viscous effects begin to play a more important role than momentum or inertial forces when scaling down geometrical dimensions. Therefore, a fluid like water will behave more like honey when it is flowing in a microscopic channel due to the fact that viscous forces are dominant to inertial forces. The fact that fluids exploit different physical properties when confining them to channels on the micrometer scale makes them useful for various applications such as cell sorting, mixing of chemical solutions and formation of chemical gradients etc. All applications making use of fluids in microscopically confined containers or channels belong to the field of microfluidics. Following sections will treat some basic concepts in microfluidics that are important for both understanding and making use of microfluidics for a certain application. [11]

2.2.2 Navier-Stokes Equation: Newton's second law of mechanics for fluids

There is a mathematical model describing fluid flow for any type of fluid and any type of conduit such as a microchannel or a tube. This mathematical model is a differential equation named *Navier-Stokes equation* and it can simply be described as Newton's second law of mechanics for fluids. The equation takes the following form for incompressible fluids:

$$\rho[\partial_t \mathbf{v} + \underbrace{(\mathbf{v}\cdot\nabla)\mathbf{v}}_{\text{inertial term}}] = -\nabla p + \underbrace{\eta\nabla^2\mathbf{v}}_{\text{viscous term}} + \underbrace{\rho\mathbf{g} + \rho_{el}\mathbf{E}}_{\text{body forces}} \tag{1}$$

where:

ρ = density of fluid $[\frac{kg}{m^3}]$
$\mathbf{v}$ = velocity field $[\frac{m}{s}]$
p = pressure $[Pa]$
η = dynamic viscosity of fluid $[Pa \cdot s]$
$\mathbf{g}$ = gravitational acceleration $[\frac{m}{s^2}]$
ρ_{el} = electric charge density $[\frac{C}{m^3}]$
$\mathbf{E}$ = electric field $[\frac{V}{m}]$

A general solution for equation 1 has never been found. It is explained by the mathematical difficulties that arise when the non-linear inertial term is included. Fortunately, the non-linear term is generally negligible in microfluidics as flow velocities are low in comparison to macroscopic flows. Further simplifcations of equation 1 are possible for

flows on the microscopic scale. Body forces are generally very small and can be excluded. The incompressibility condition further gives:

$$\partial_i v_i = 0 \tag{2}$$

Navier-Stokes equation is thus simplified to a linear expression making analytical solutions possible:

$$0 = -\nabla p + \eta \nabla^2 \mathbf{v} \tag{3}$$

Solutions to equation 3 are stationary and do not account for flows developing over time. For time-dependent flows it is neccessary to include the time derivative $\partial_t \mathbf{v}$ in equation 1 yielding the linear time-dependent Navier-Stokes equation [12]:

$$\rho \partial_t \mathbf{v} = -\nabla p + \eta \nabla^2 \mathbf{v} \tag{4}$$

2.2.3 Scaling Laws and Reynolds Number

A fluid which is contained in a microchannel will experience more surface forces than a fluid in a macroscopic channel such as a river. It can be explained by the basic scaling law in microfludics:

$$\frac{surface forces}{volume forces} \propto \lim_{l \to 0} \frac{l^2}{l^3} \to \infty \tag{5}$$

Surface forces scale down as the square of a certain channel length l while volume forces scale as the cube of l which can be seen in equation 5. As l decreases in magnitude when scaling down geometrical dimensions, surface forces will begin to dominate over volume forces. [12]

The correlation given by 5 has implications on the flow of a fluid. In microchannels, the fluid tends to flow in infinitesimal parallel layers without any disturbance between them, see figure 6a. It is a result of the increasing impact of viscous effects arising when surface forces dominate. This type of flow is known as *laminar flow*. Occurence of laminar flow at the microscopic scale is often desirable in microfluidics since the flow is deterministic and enables sorting of for example particles and cells or controlled mixing of chemical solutions. [11] In contrast, when volume forces dominate the flow there is a considerable disturbance between the fluid layers as vortices easily are initiated. A typical property of turbulent flow is spatially disordered velocity fields which fluctuates randomly in time, see figure 6b. [13] There is a dimensionless number called *Reynolds number*(Re) giving a quantitative estimation of whether a fluid will be laminar or turbulent. Reynolds number is derived from Navier-Stokes equation where its magnitude determines if the flow for a certain fluid will be principally described by the inertial term or the viscous term of the equation. A general equation for Reynolds number is given by:

$$Re = \frac{\rho u L}{\eta} \tag{6}$$

where:

ρ = density of fluid $[\frac{kg}{m^3}]$
u = flow speed $[\frac{m}{s}]$
L = characteristic length $[m]$
η = dynamic viscosity of fluid $[Pa \cdot s]$

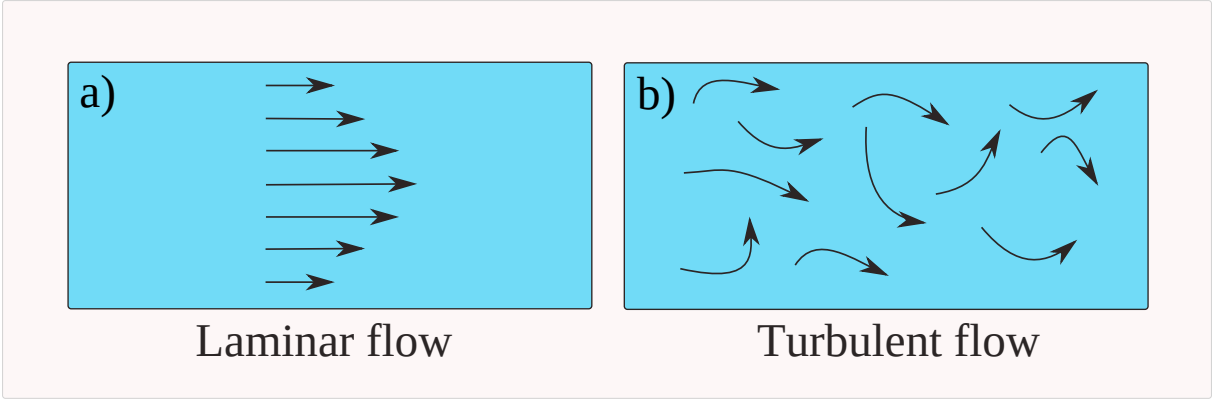

Figure 6: *a) Fluid layers flow parallel in infinitesimal layers without any disturbance between them. b) Fluid layers flow in a unordered manner with considerable disturbance between them as vortices are easily created.*

For lower values of Reynolds number ($Re < 1500$) the viscous term dominates the inertial term in Navier Stokes equation, see equation 1, and the flow is laminar. As seen in the numerator of equation 6, low flow speeds, small channel dimensions and low densities yield lower values of Re. From the denominator it is given that high viscosities yield lower Re. In case of high Re($Re > 2500$), the inertial terms dominates the viscous term and the flow is turbulent. [12] [14] As an example, Re can be estimated for a circular tube having a diameter(characteristic length) of 100 μm. If water is flowing in the tube with a flow of 100 $\mu l/h$, then Re number is given by:

$$Re = \frac{\rho u L}{\eta} = \frac{1{*}10^{3}{*}[\frac{kg}{m^3}]{*}2.1{*}10^{-1}{*}[\frac{m}{s}]{*}100{*}10^{-6}[m]}{1{*}10^{-3}[Pa{\cdot}s]} = 21.2 \tag{7}$$

The flow in this circular tube is thereby laminar as Re < 1500.

2.2.4 Péclet Number

Many microfluidic chips utilize both convective transport and diffusional transport of solutes, see figure 7. When solutes are carried with the fluid that flows in the microchannel, it refers to convective transport. However, solutes also move randomly in the fluid as they collide with molecules constituting the fluid. This random movement is known as diffusion. [11] In order to determine whether transport is dominated by diffusion or convection it is necessary to estimate the Péclet number. The formula for this dimensionless number is given by:

$$Pé = \frac{\textit{diffusion time}}{\textit{convection time}} = \frac{\tau^{rad}_{diff}}{\tau^{a}_{conv}} = \frac{\frac{a^2}{D}}{\frac{a}{V_0}} = \frac{V_0 a}{D} \tag{8}$$

where:

τ^{rad}_{diff} = time to move the distance a by radial diffusion $[s]$
τ^{a}_{conv} = time to move the distance a by axial convection $[s]$
a = distance $[m]$
D = diffusion coefficient for solute $[\frac{m^2}{s}]$
V_0 = flow velocity $[\frac{m}{s}]$

With a high Pé the transport of solutes is predominatly due to convection. As seen in equation 8, high flow velocities, large distances and small diffusion coefficients yield high Pé. Small Pé imply that transport occurs mainly by diffusion. It is dominant for small distances, low flow velocities and large diffusion coefficients. Flow velocities and distances are generally small in microfluidics which often results in small Pé. [12]

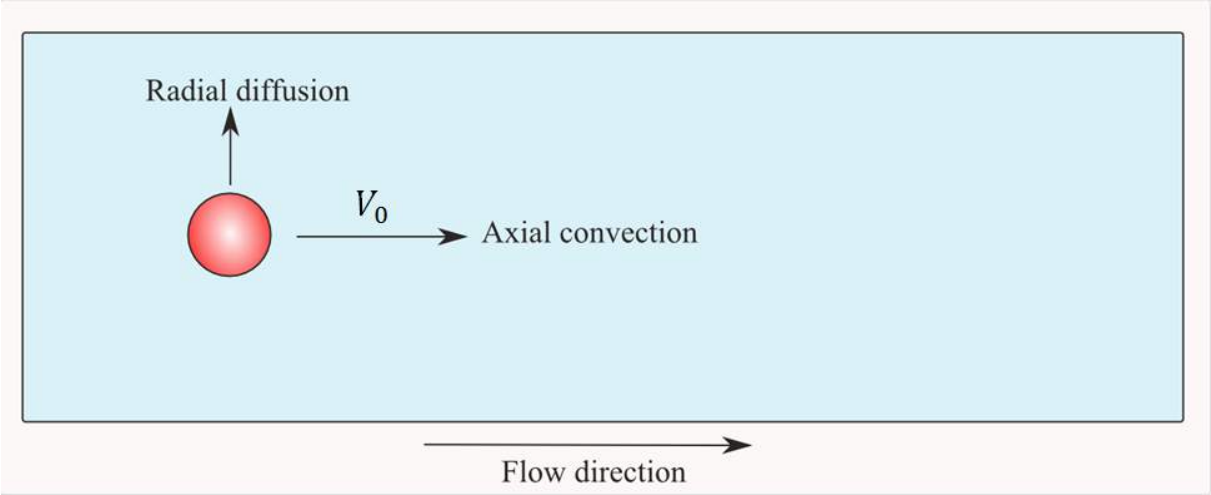

Figure 7: *A particle moves in a fluid due to both convective and diffusional transport. In this case, the flow velocity* V_0 *is high and diffusional transport is small as indicated by the arrows. It results in a high Pé.*

.

2.3 Generating gradients in a microfluidic system

2.3.1 Flow-based gradient generators

A concentration gradient is generated perpendicular to the flow direction in a microfluidic gradient generator, see figure 8. In the same figure there are two fluids with different concentrations of a substance such as 1 mol/m^3 and 0 mol/m^3 that are injected at each inlet with identical flow rates. A concentration gradient is formed as the two fluids are repeatedly mixed in the channel network. The concentration gradient is spatially and temporally stable due to the prevailing laminar conditions in the microchannel network and the continuous flow where infusion and withdrawal of fluid and substances are balanced. In order to ensure specific and homogeneous concentrations in each mixing channel

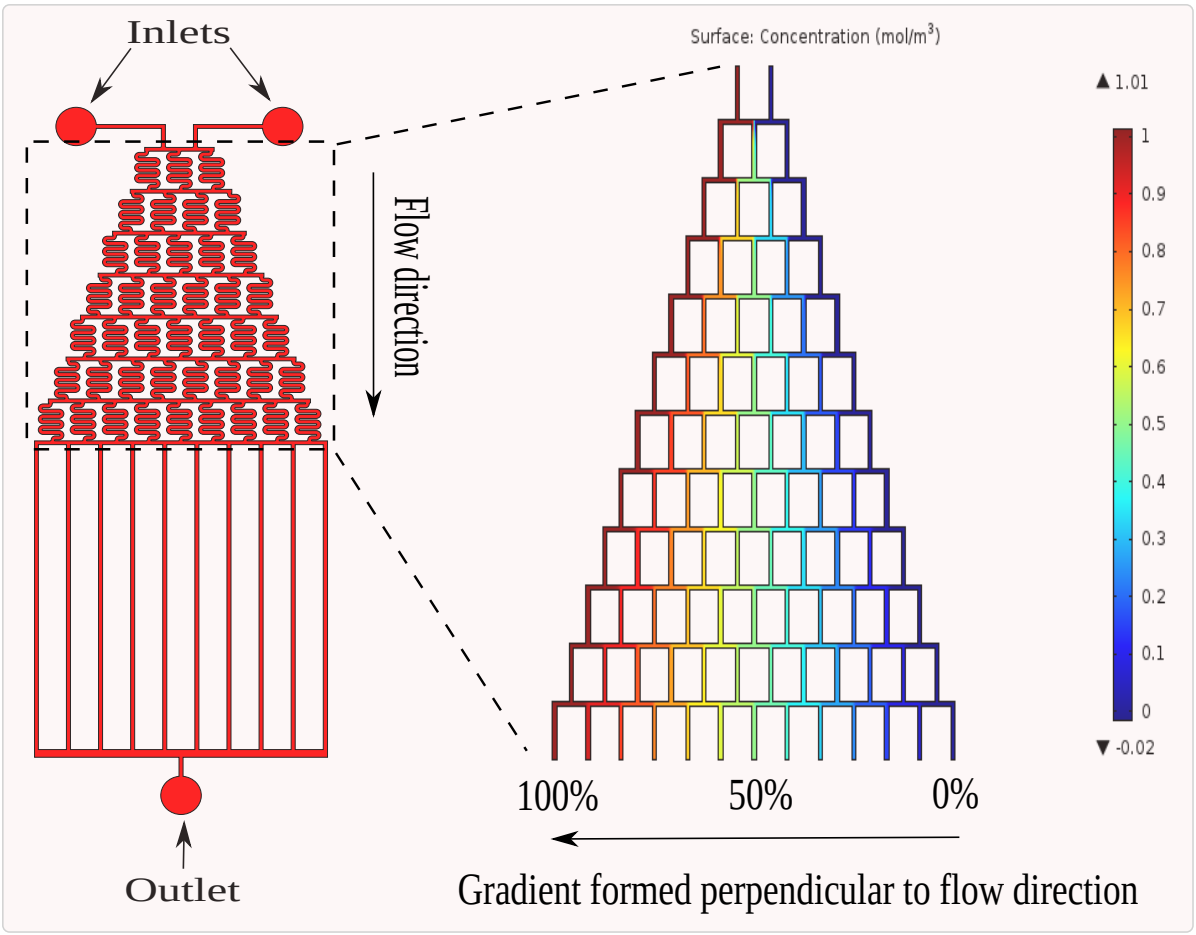

Figure 8: *Schematics over a flow based gradient generator. The serpentine region is modeled in COMSOL to show the mixing procedure and the final concentration gradient.*

before splitting, it is necessary to govern the Péclet number. For a microfluidic gradient generator a low Pé is preferable since mixing and thus gradient formation relies on diffusion of solutes between laminar streams. From observing equation 8 it is realized that the diffusion time for the substance must be sufficient to ensure proper mixing. Judging from the same equation, it implies that either flow velocities must be set to be low enough or diffusion distances must be small. Even if flow velocities are set low it is important to consider the design and dimensions of the gradientgenerator. By designing long mixing channels solutes will have more time to diffuse a certain distance in comparison to a shorter mixing channel. An approach for making longer channels while restricting the size

of the gradient generator, is to design serpentine-shaped channels, see figure 9. As stated above, mixing channels should also be designed to have a limited width to compensate for the diffusion distance. [15] [16]

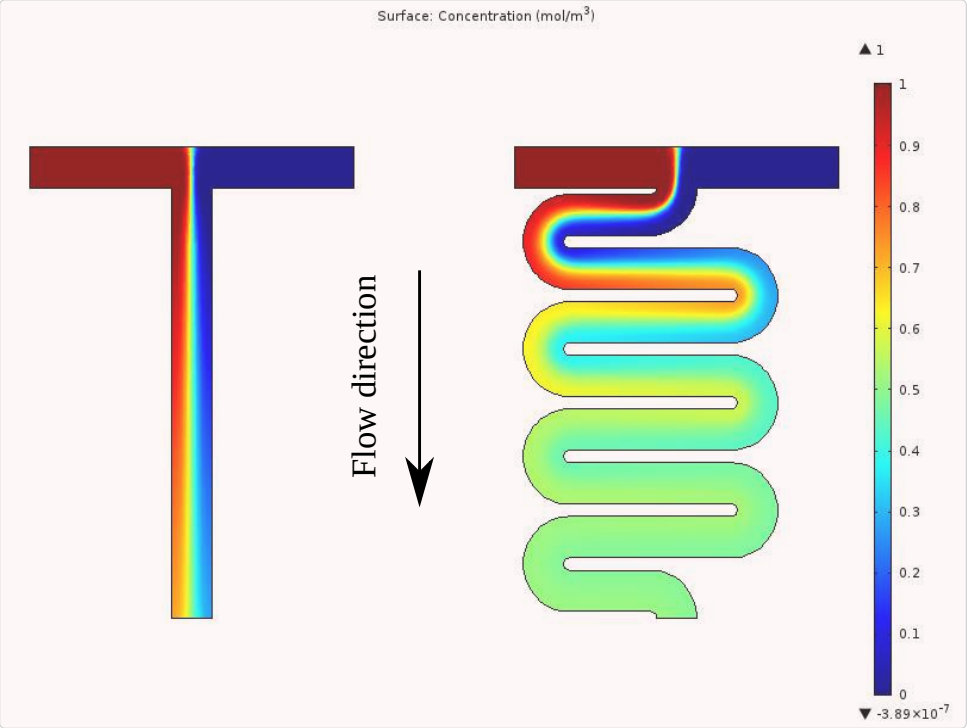

Figure 9: *Straight channels versus serpentine channels. By making serpentine channels it is possible to ensure that two fluids with different concentrations are completely mixed. Seen in the end of the straight mixing channel, it is not a homogeneous concentration but a gradient across the width channel. Except for ensuring a homogeneous concentration, serpentine channels also save space on the microfluidic chip.*

2.3.2 Determining concentrations in a flow-based gradient generator

A gradient generator is capable of generating different concentration profiles. In applications utilizing gradient generators, a particular concentration profile might be preferred over others. It emphasizes the importance of understanding how to calculate and derive the concentrations formed at the outlets. Fortunately, many hydraulic circuits can be analyzed as electrical circuits and it also applies to the gradient generator. A correlative electrical circuit for the gradient generator is seen in figure 10. Horizontal resistances have been neglected due to the fact that vertical resistances R_V generally have a much higher magnitude. It is an approximation based on the difference in length between vertical channels and horizontal channels. By using this approximation it is possible to deduce the flow splitting at each junction or node. If an index system is introduced, any node in the gradient structure can be descibed by two separate index notations, B and V. Index B represents the number of vertical channels at certain level in the gradient generator. Index V represents the actual vertical channel counted from left to right, starting with zero.

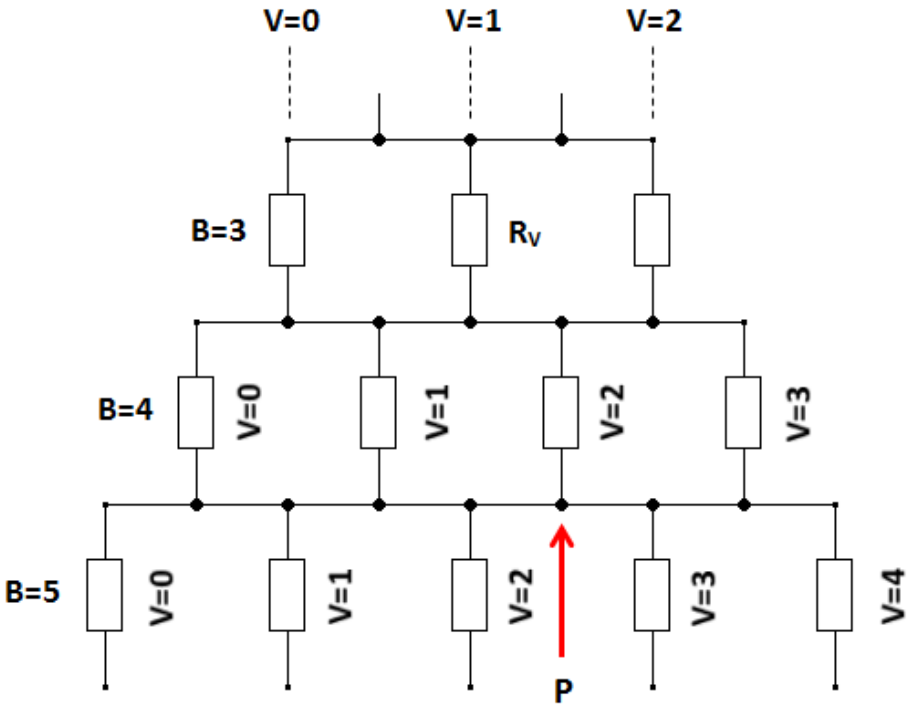

Figure 10: *Equivalent electrical circuit for the gradient generator.*

By using the following formulas, the flow splitting at a certain node is determined by:

$$S_{BV}^{R} = \frac{V+1}{B+1} \tag{9}$$

$$S_{BV}^{L} = \frac{B-V}{B+1} \tag{10}$$

where:

S_{BV}^{R} = Fraction of incoming flow going right at the junction denoted by BV
S_{BV}^{L} = Fraction of incoming flow going left at the junction denoted by BV

At node P, see figure 10, the flow splitting is determined by inserting the proper indices into equation 9 and 10:

$$S_{BV}^{R} = S_{42}^{R} = \frac{3}{5}$$

$$S_{BV}^{L} = S_{42}^{L} = \frac{2}{5}$$

The concentration in a serpentine channel is determined by first dividing the flow ratio from each recombining stream with a factor B/(B+1), multiply it with its initial concentration and then sum the result, see figure 11. In this figure, C_x, C_y and C_z correspond to different concentrations while V_x, V_y and V_z are vertical channel indices as compared to figure 10.

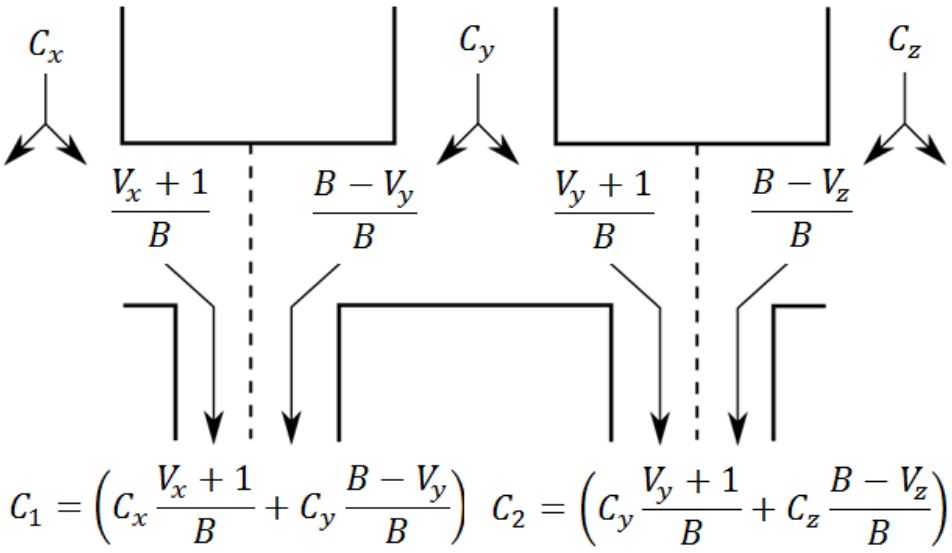

Figure 11: *Generation of new concentrations. Two laminar streams with different concentrations recombine, mix and form a new intermediate concentration depending on the flow splitting ratio.*

As an example we can consider node P again and set following values:

$$C_x = 1[\frac{mol}{m^3}] \qquad V_x = 1$$
$$C_y = 5[\frac{mol}{m^3}] \qquad V_y = 2$$
$$C_z = 10[\frac{mol}{m^3}] \qquad V_z = 3$$

If the flow splitting for node P is taken into consideration and the flow splitting for the neighbouring nodes are calculated, we obtain the following result:

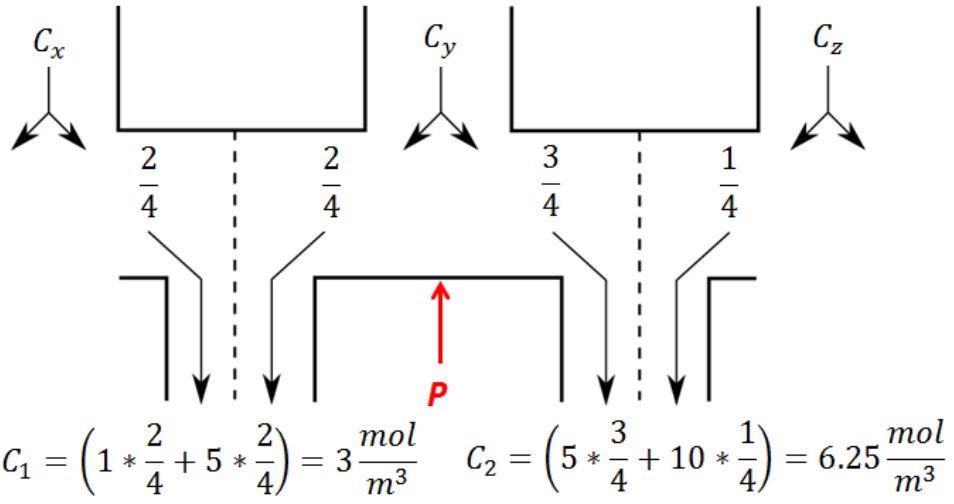

Figure 12: *Concentrations generated at node P and its vicinity.*

2.3.3 Soft lithography for fabrication of microchannels

Soft lithography is a set of microfabrication techniques utilizing an elastomer as a stamp, mold or mask. A common elastomer is *poly(dimethylsiloxane)*, abbreviated PDMS. This elastomer has some properties suitable for a microfluidic device. It can be made optically transparent, which enables optical observation of cell cultures and fluorescence microscopy. It is flexible which makes it robust and does not require cautious handling. PDMS is also biocompatible which is an advantage when fabricating a cell culture system. A PDMS stamp is created by pouring uncured liquid PDMS on a master with relief structures on the surface. The master/PDMS assembly is then usually inserted into an oven for curing. During the curing process, PDMS is crosslinked and becomes solid. After curing, the solid PDMS stamp can be removed from the master using a scalpel and a tweezer, see figure 13. The stamp will then have the inverse relief structures of the master and can be used for either microcontact printing or sealed against a flat substrate such as glass or another flat PDMS surface. When sealing a microfluidic device the latter case is used. Channels are patterned in the stamp and sealed against a flat substrate to enclose the channels. [17] [18]

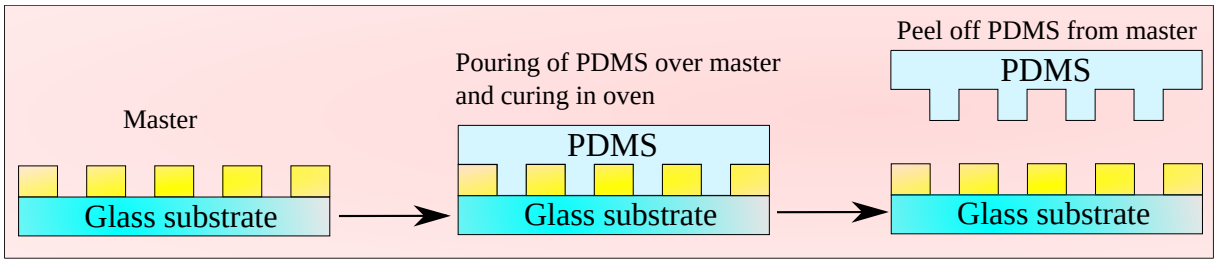

Figure 13: *Steps in soft lithography. PDMS is poured on a fabricated master having resist patterns. As the PDMS/master assembly is cured in an oven the PDMS becomes solid. After curing, it is possible to peel off the PDMS stamp from the master.*

3 Project background and research questions

This master thesis project is based on an earlier project about creating a microfluidic device capable of differentiating hESCs. This device will constitute a biomimetic system which will imitate the rostro-caudal patterning of the neural tube. Instead of WNT, *Glycogen synthase kinase 3* enzyme inhibitor (GSK3i) is used as morphogen since it is more effective and easier to handle. The microfluidic device should be capable of generating a gradient of GSK3i and have an integrated cell culture chamber. Following schematics, see figure 14, show the design of the first microfluidic device: Figure 14a shows the top

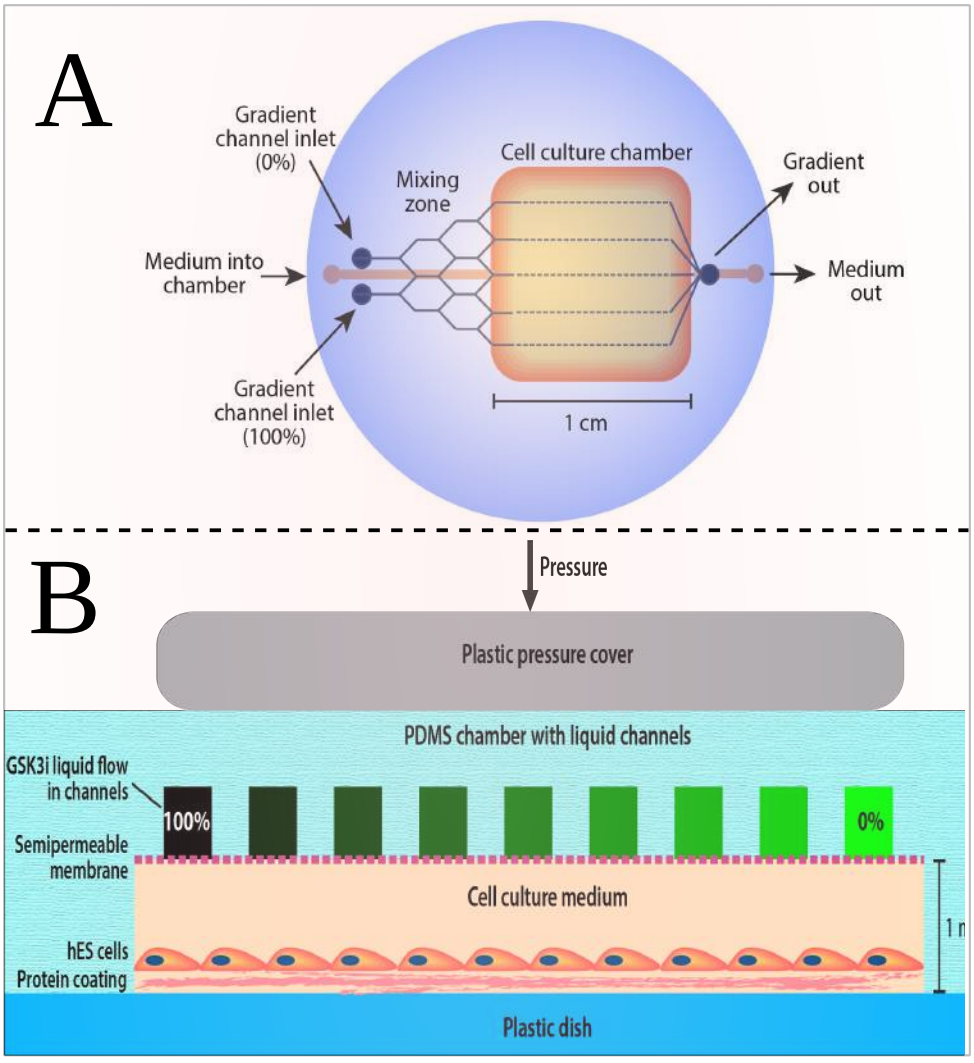

Figure 14: *Schematics of first microfluidic device A) Top-view of the microfluidic device. B) Cross-sectional view of the microfluidic device.*

view of the device. It consists of three layers: a gradient generator PDMS stamp, a polycarbonate semipermeable membrane and a cell culture stamp. These layers are displayed more clearly in figure 14b, illustrating the cross-sectional view of the device. The main idea behind this design is that the generated concentration gradient of GSK3i molecules in the different channels will diffuse through the semipermable membrane into the cell culture chamber. Cells along the width of the channel will be subjected to different local concentrations of this morphogen and thereby different cell types will be generated.

A new device will be designed using the same mechanism as the chip in the figure above. But it will be designed with some new specifications:

1. A wider culture chamber must be fabricated to allow for more cell types. The width should be increased from 1 cm to 2 cm while the channel length of 1 cm is preserved as well as the channel height of 1 mm.

2. A new gradient generator with more vertical channels must be fabricated to cover the width of the new culture chamber.

3. A new device holder must be fabricated to ensure proper contact between the device and the cell culture dish. Cell medium might otherwise leak out from the culture chamber.

Research questions

Some questions will constitute the framework for this project and guide in the creation of a developing-brain-on-a-chip:

1. Prior to fabrication, can a 2D simulation of the gradient generator and the culture chamber be performed to evaluate the flow behavior in these designs?

2. Is it possible to fabricate a second generation flow based gradient generator and a culture chamber in PDMS using soft lithography?

3. Can the fabricated PDMS stamps be bonded with a semipermeable membrane in between to form a functional microfluidic device?

4. Is it possible to differentiate human embryonic stem cells into cell types of forebrain, midbrain and hindbrain along the rostro-caudal axis?

4 Method

4.1 Simulations

Simulation software *COMSOL Multiphysics 4.4* was used to understand the flow behavior and the gradient formation in microfluidic gradient generators. The *laminar flow physics module* was chosen since microfluidic devices have these conditions. For this module, COMSOL uses the finite element method to solve Navier-Stokes equation, (see equation 3) numerically in mesh nodes. Solutions were then illustrated in different graphs such as 2D surface graphs or 1D graphs.

4.1.1 First generation gradient generator

The first generation gradient generator was drawn using the inherent CAD function of the software. It had the same design as the first gradient generator used initially in the project. Water was chosen as material for the model and necessary boundary conditions were made. A physics controlled mesh had to be applied to the model and only the normal mesh was chosen. Having a finer mesh results in a higher resolution but the simulation takes longer time to solve as more mesh nodes are added. The velocity magnitude for the first generation gradient generator was then simulated and plotted. In order to understand the gradient formation another physics module: *transport of diluted species* was added to the model. A concentration of 1 $\frac{mol}{m^3}$ was chosen for one of the two inlets while a concentration of 0 $\frac{mol}{m^3}$ was chosen for the other inlet. An arbitrary substance having a default diffusion coefficient of $1{*}10^{-9}\frac{m^2}{s}$ was chosen in the module. This value would ensure that concentration equilibrium would prevail in each mixing channel. After setting these parameters, another simulation was performed and a concentration surface graph was plotted.

4.1.2 Second generation gradient generator

Similary to the first model, a 2D geometry of design C, see mask template, was drawn and the same setting were made. Both the velocity magnitude in the gradient generator and a concentration surface graph were plotted.

4.1.3 Culture chamber

A culture chamber design was simulated in 2D to see whether the flow in the culture chamber part would be homogeneous. It is desirable that all cells in the culture chamber have the same flow as the concentration gradient might be affected. The flow velocity magnitude was plotted in a surface graph.

4.2 Fabrication of microfluidic device

4.2.1 Master fabrication

A gradient generator master was fabricated using UV lithography, see figure 15. As UV

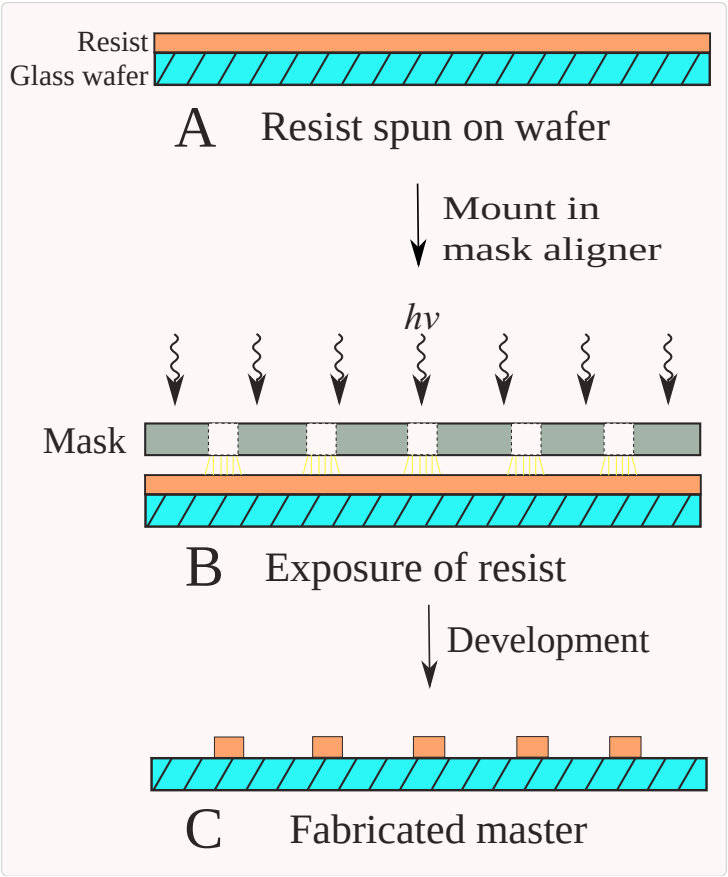

Figure 15: *Main steps in UV lithography. A) Negative resist is applied on a glass wafer and spun to form an even layer on the surface. B) The soft-baked resist is exposed to UV light through the mask resulting in crosslinking of the resist. C) Only crosslinked exposed areas of the resist remain after development while unexposed areas are washed away during the devlopment.*

lithography requires a mask, it was necessary to fabricate a mask with the gradient generator patterns. Therefore a mask template was designed with the CAD software AutoCAD 2013. Four variations of gradient generators were created to fit in a 4 inch mask, see figure 16. Channel widths of 100 μm and 200 μm were chosen as these values are rather standard when designing microfluidic channels. For design A)/B) the length of a single serpentine equals 3.78 mm while the serpentine length for design C)/D) equals 2.70 mm. The vertical channel region for all designs equals 1.2 cm.

The mask template was converted from the standard CAD drawing file(.dwg) to a drawing exchange format file(.dxf) which was read by the mask writer software. Gradient generator designs were printed on a 4 inch chromium mask substrate from the template file using a mask writer (Heidelberg Instruments DWL66). The mask was completed with wet chromium etching in a clean room , see appendix A1 for the protocol. In figure 17, the fabricated mask is shown.

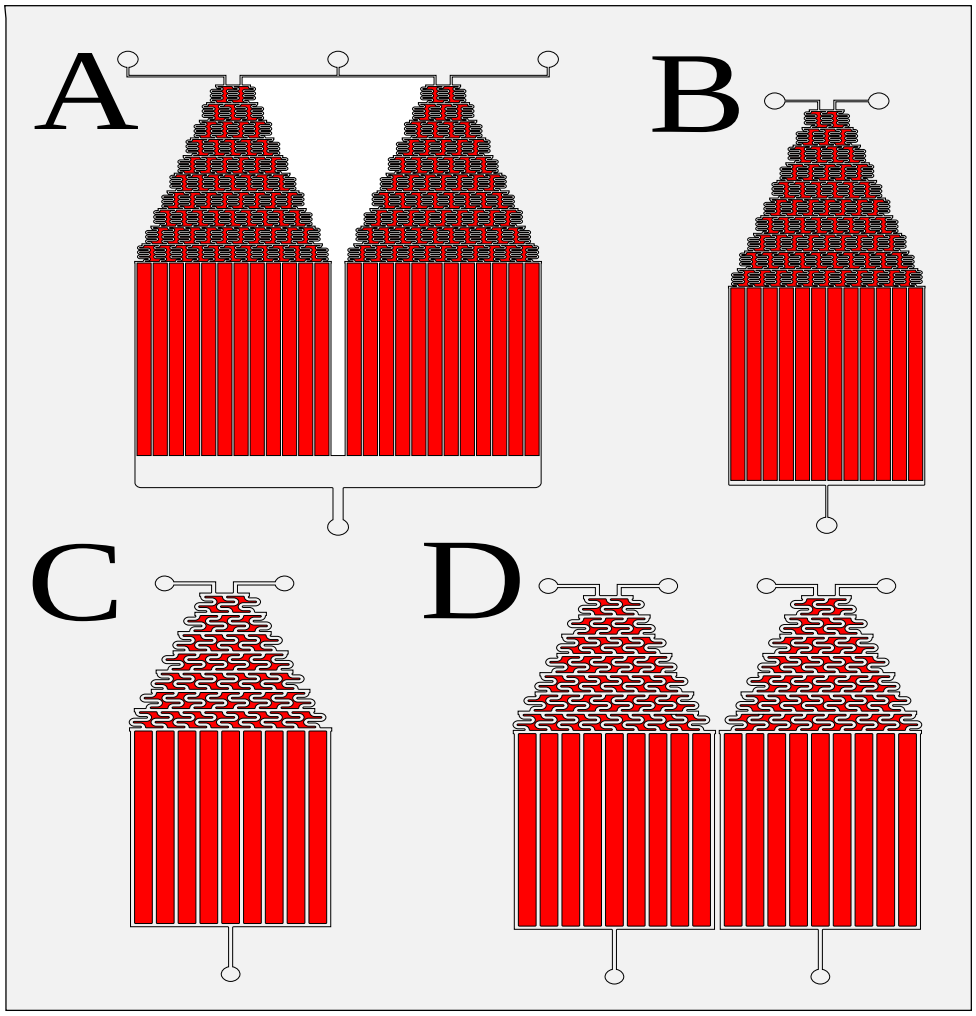

Figure 16: *Mask template with four different gradient generator designs made in AutoCAD. Design A) and B) have 100µm wide channels while design C) and D) have 200µm wide channels.*

A negative photoresist (AZ EXP 125nXT-10A, AZ Electronic Materials) was spun onto a clean 4 inch glass wafer, see figure 15a. The resist had a thickness of approximately 100 μm after using an established spin protocol, see appendix A2. Soft baking of the resist followed to remove the solvent from the resist. The mask was placed on top of the baked resist with the chromium side in direct contact with the resist. The wafer with the attached mask was then placed on a sample holder of a mask aligner (Karl Suss Mask Aligner MA4) and the resist was exposed to UV light for 7 minutes, see figure 15b and appendix A3. After exposing the resist, it was developed using a specific developer (AZ 326 MIF Developer, AZ Electronic Materials) to form the complete master, see figure 15c. For a more detailed protocol of the development process, see appendix A4 .

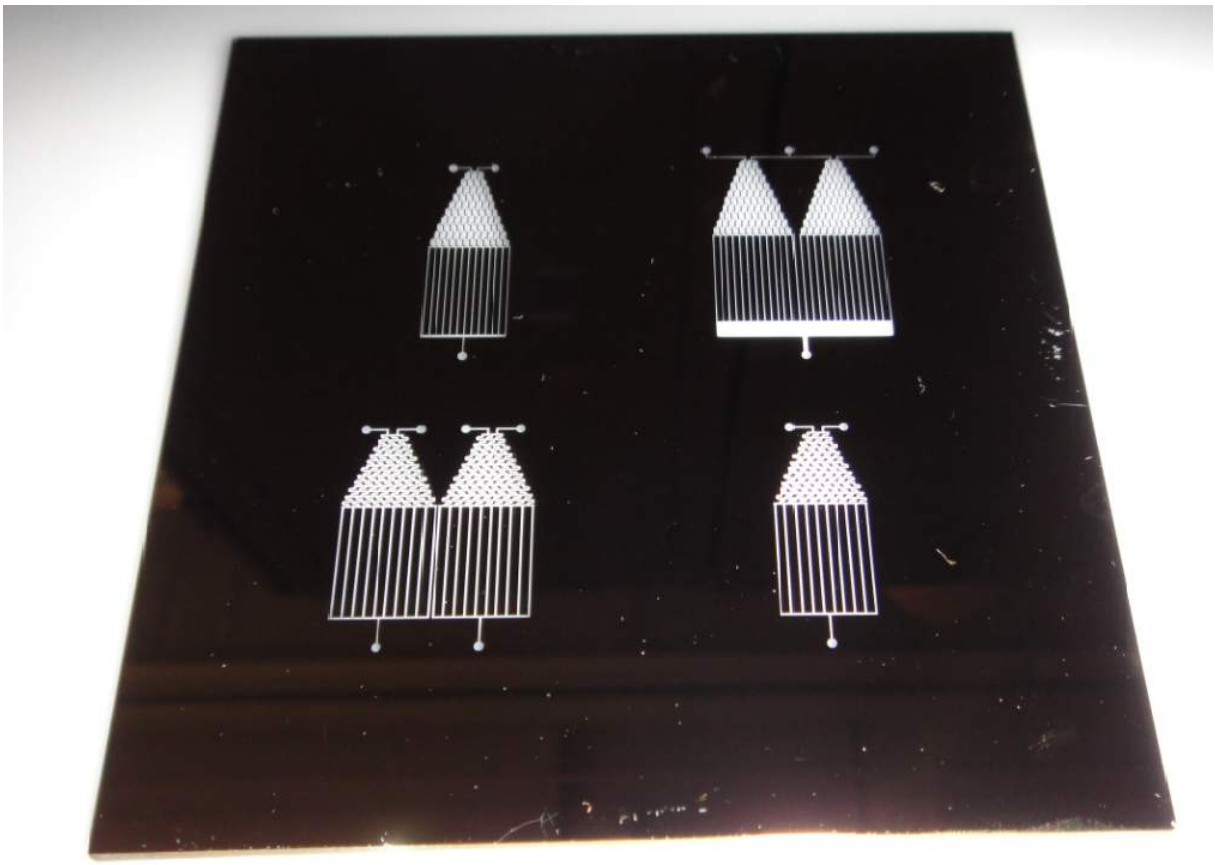

Figure 17: *Fabricated chromium mask from the drawing exchange format file.*

4.2.2 Injection mold fabrication

A PDMS injection mold for fabrication of a culture chamber stamp was designed using a CAD/CAM/CNC(Computer Aided Design/ Computer Aided Manufacturing/ Computerized Numerical Control) software package called *Galaad*. The software was used together with a CNC milling machine (ICP 4030, ISEL) to mill details in plastics from the CAD model. Dimensions for the culture chamber details of the mold can be seen in figure 18.

Once completing the CAD-drawing, milling depths and cutting tools had to be set for every drawn object in the Galaad file. The milling procedure was first simulated in Galaad to ensure that objects would be milled according to the settings made. For a detailed description of how to make these settings, see the instruction manual [19]. A sheet of transparent plastic material (2mm, PMMA) was attached to the milling board using vacuum and a cutting tool was mounted inside the milling machine. Air cooling was directed towards the milling head to avoid melting the plastics while milling. After calibrating the milling head, the milling was initiated in Galaad. In figure 19, the milling process can be seen.

Every 15 minutes, the milling procedure was checked to ensure the plastic material had not been released from the vacuum nor the cutting tool had been broken. After milling and cutting out an area of 78*78 mm^2 from the plastic sheet, the injection mold was taken out from the milling machine and put in an ultrasonic bath to remove small plastic residues.

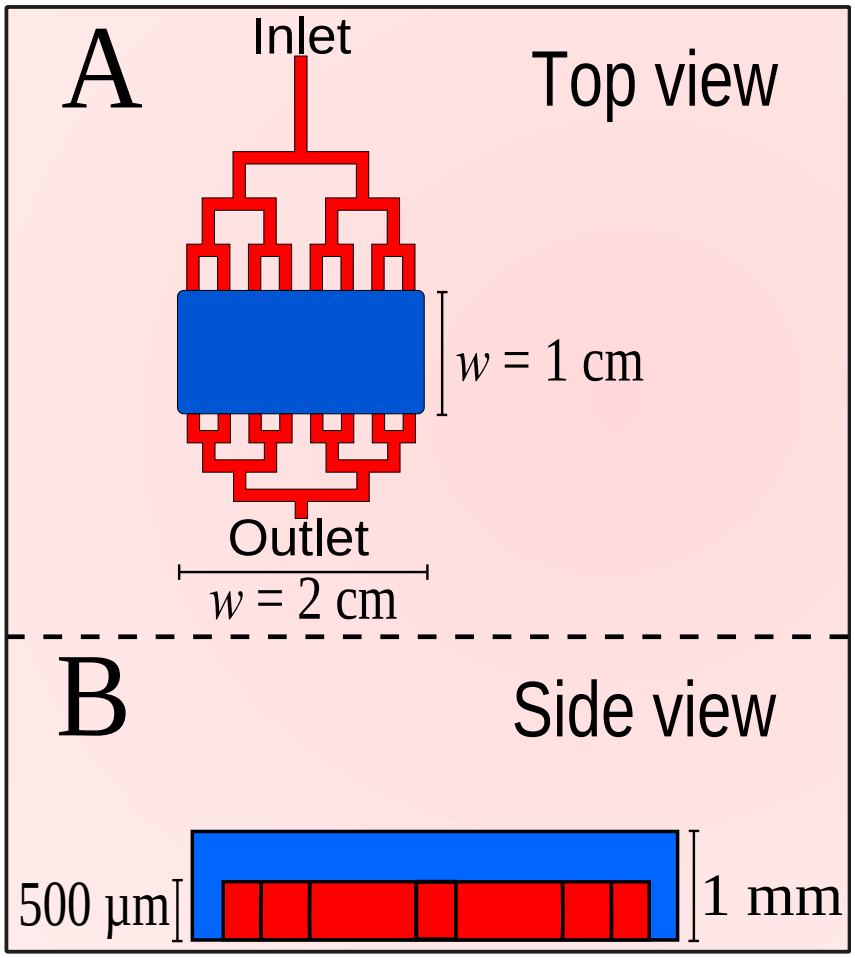

Figure 18: *Dimensions of the culture chamber. A) Top view of the culture chamber. The width of the culture chamber seen in blue is designed to have a width of 2 cm and a length of 1 cm. The branched inlet channels and outlet channels are seen in red. They should ensure an even flow profile in the culture chamber.B) Side view of the culture chamber. For the inlet channels and outlet channels, the height equals 500 µm while the height of culture chamber equals 1 mm.*

4.2.3 Soft lithography

Gradient generator stamp

In order to facilitate the later lift off process of the PDMS stamp, a thin coating of polyvinyl alcohol(PVA) had to be applied to the master. PVA is commonly used as a sacrificial layer for low stress releases of PDMS layers from substrates [20]. An aqueous solution of PVA was first prepared in a falcon tube(BD Falcon, 50 ml), see appendix B1. The surface of the master was made hydrophilic using a plasma asher (Diener Plasma Asher), see appendix B2, and then dipped into 15 ml of PVA solution. After dipping the master, it was directly placed in an oven to evaporate the water. A thin PVA coating could later be seen in the microscope, see figure 20.

PDMS was mixed and prepared in a petri dish according to appendix B3. It was then poured on the master lying in the bottom of another petri dish until it was completely covered. The covered master in the petri dish was then put in a vacuum dessicator for 1.5 h to remove bubbles, known as degassing, and make it completely transparent. After

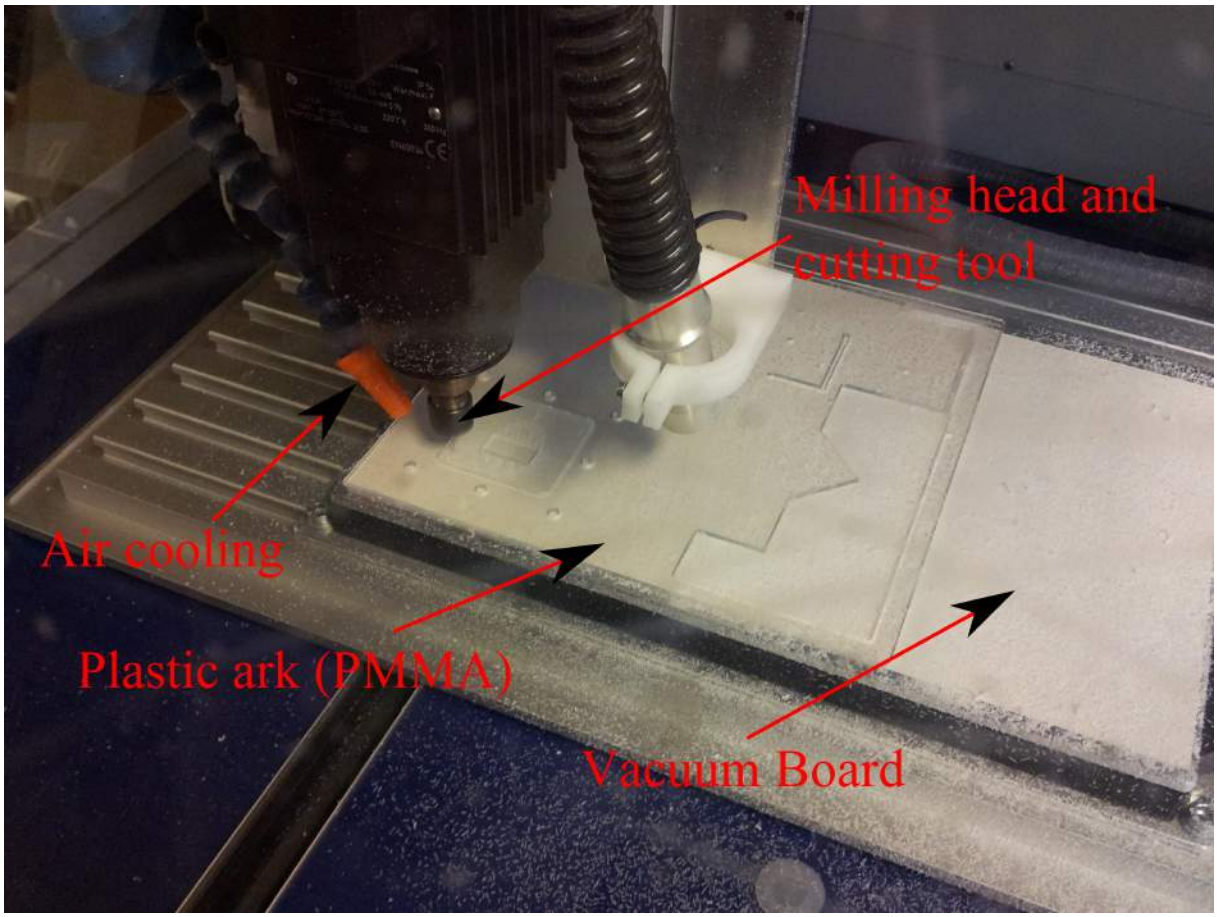

Figure 19: *Milling of the culture chamber PDMS mold. Air cooling is directed towards the area where the cutting tool mills the plastic material to avoid melting and potential damage to the cutting tool. The vacuum board fixes the plastic sheet during the milling process.*

degassing, the petri dish was put in an oven for curing (60°C, 2 h).

The PDMS stamp was after curing removed from the master by first using a sharp scalpel to cut a rectangular area of interest. Some Milli-Q water was then poured into the petri dish to facilitate the peel off. The PDMS stamp was gradually removed from the master by lifting one of the cut-out edges with a wafer tweezer. When lifting one side of the stamp, water could enter in the interface between the master and the stamp to dissolve PVA. By gently pulling the stamp off the master, the risk of tearing the PDMS would be minimized and water would have enough time to dissolve PVA.

When the stamp was removed from the master, it was studied under microscope to see whether some details were torn or if PVA residues were present. In case of PVA residues, the stamp was washed properly in Milli-Q water and then repeatedly studied in microscope.

Injection mold stamp

PDMS (10g base, 1:10) was mixed and prepared according to protocol, see appendix B3, and degassed in a vacuum dessicator until the PDMS mixture was transparent. A

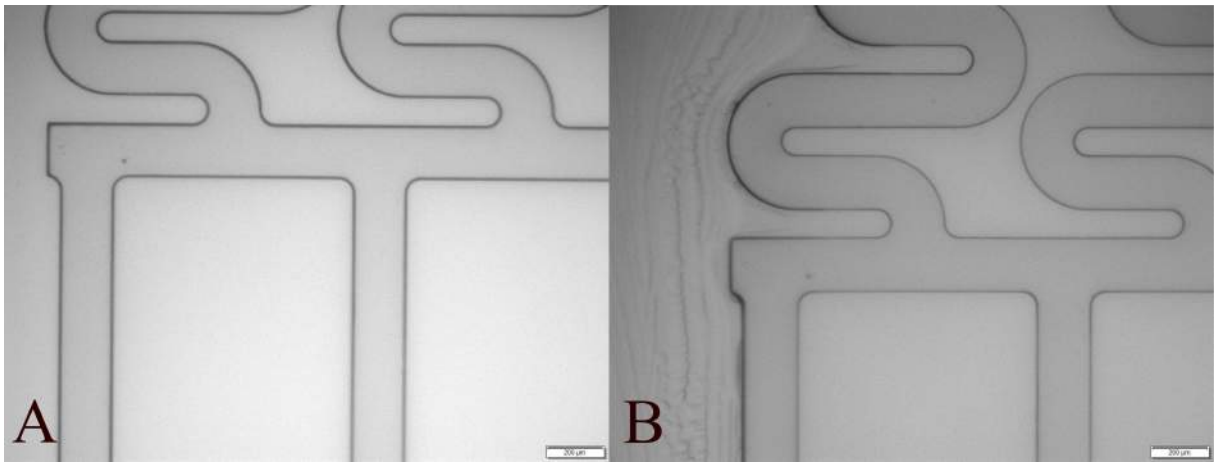

Figure 20: *Part of master studied under microscope. A) Master before PVA-treatment. B) Master after PVA treatment. Small accumulations of PVA can be seen as dark lines next to the left serpentine channel.*

syringe (5 ml, BD Plastic) was then filled with uncured PDMS and a circular syringe needle was mounted. The previously milled injection mold was assembled using 8 screws and nuts. In order to fill the mold, the syringe needle was inserted into one of the two holes made in the lid. PDMS was slowly injected manually into the mold to avoid bubble formation and until uncured PDMS had completely filled the mold, see figure 21. The mold was then cured in an oven (2 h, 60°C).

4.2.4 Cutting of inlets and outlets

Inlets and outlets must be cut in the PDMS in order to connect tubings and provide the device with cell medium. A sharp syringe needle was used to make circular 1 mm diameter inlets and outlets in the PDMS stamp, see figure 22a. As reference, the inlet/outlet marks in the PDMS were used. Cut inlet and outlet holes were properly cleaned with water to remove PDMS residues that potentially could clog the microchannels. Also nitrogen gas was used to control that no residues were present.

4.2.5 Bonding of device

A clean 4 inch glass wafer was mounted with vacuum in a spinner. PDMS (1ml) was spun until a thin layer was covering the entire wafer, see appendix C1. The gradient generator stamp was bonded to the semipermeable membrane(polycarbonate 0.2 μm pore size, Whatman) and the culture chamber stamp using uncured PDMS as glue, see appendix C2. Bonding is illustrated in figure 23.

4.2.6 Attachment of silicone connectors

Short silicone connectors were glued at the outlets/inlets using silicone glue (Elastosil A07, ELFA) for connection of teflon tubings to the device, see figure 22b. The device was then left in a petri dish with the lid partly open for the glue to dry (>6 h). The petri dish with the lid served as protection against dust which could enter the device through inlets/outlets during the drying process.

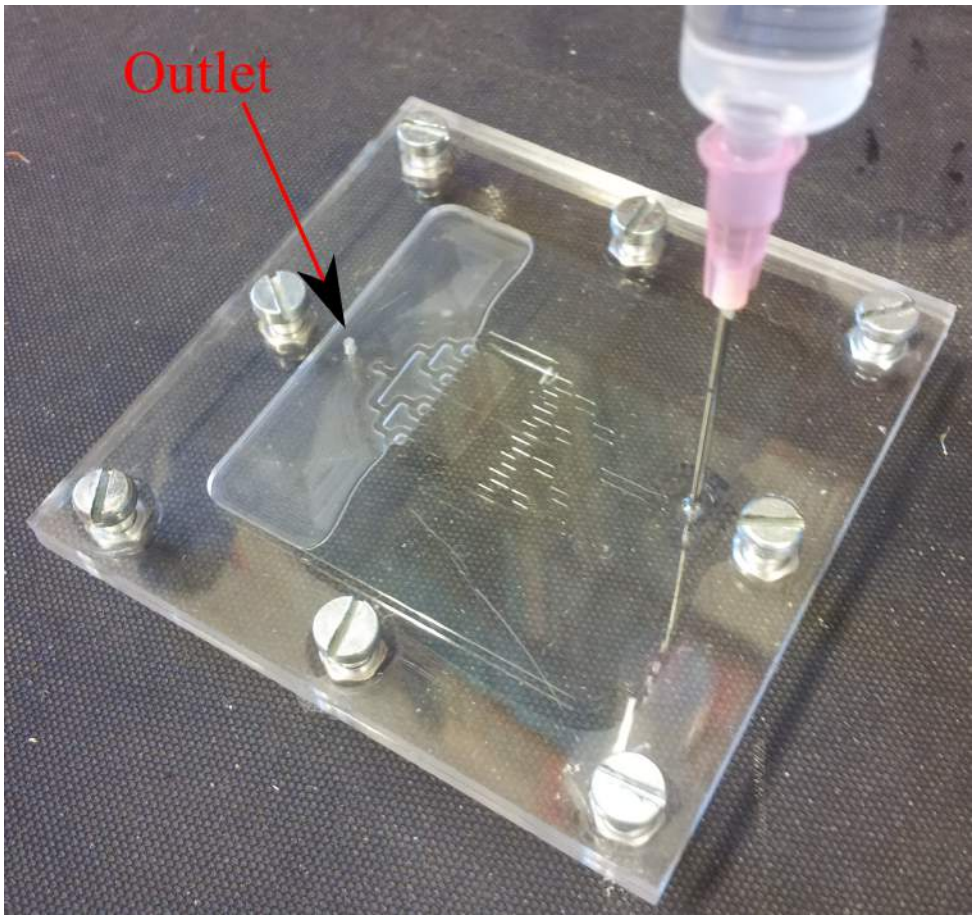

Figure 21: *Injection of uncured PDMS into the assembled injection mold. Seen in the image, 75% of the mold is filled. By using 8 screws, the mold is sealed properly and PDMS can only exit through the outlet.*

4.2.7 Device finishing

The device must fit in a 6 cm diameter cell culture dish (NUNC, 60 mm), referred to as plastic dish in figure 14b. Therefore it is necessary to use a scalpel to cut away PDMS pieces from the device until it fits in the cell culture dish. By placing the device on top of the culture dish, it is possible to use a pen to mark the areas which need to be cut away in order to get an optimal fit of the device inside the NUNC dish.

4.3 Device holder fabrication

A holder to ensure a tight connection between the device and the cell culture dish needed to be constructed. A bottom piece for the holder was designed in Galaad and milled using the milling machine, similar to the injection mold. A plastic sheet(20 mm, POM) was used for the bottom piece.

In order to apply pressure from above, a lid was also made from a 20 mm POM plastic sheet. It was designed to apply an even pressure on the entire device and only have milled holes for silicone connectors. Also it needed to account for the high edges of the NUNC dish.

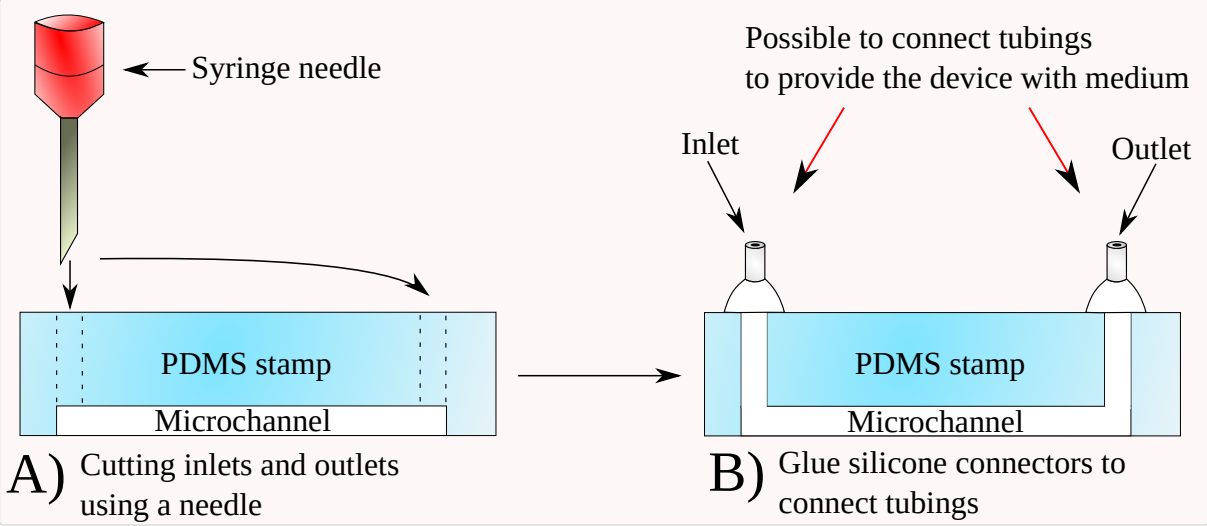

Figure 22: *A) A sharp needle is used to cut inlets and outlets in the PDMS stamp. B) Silicone connectors can be glued at the inlets and outlets to connect tubings and to provide medium to the channels.*

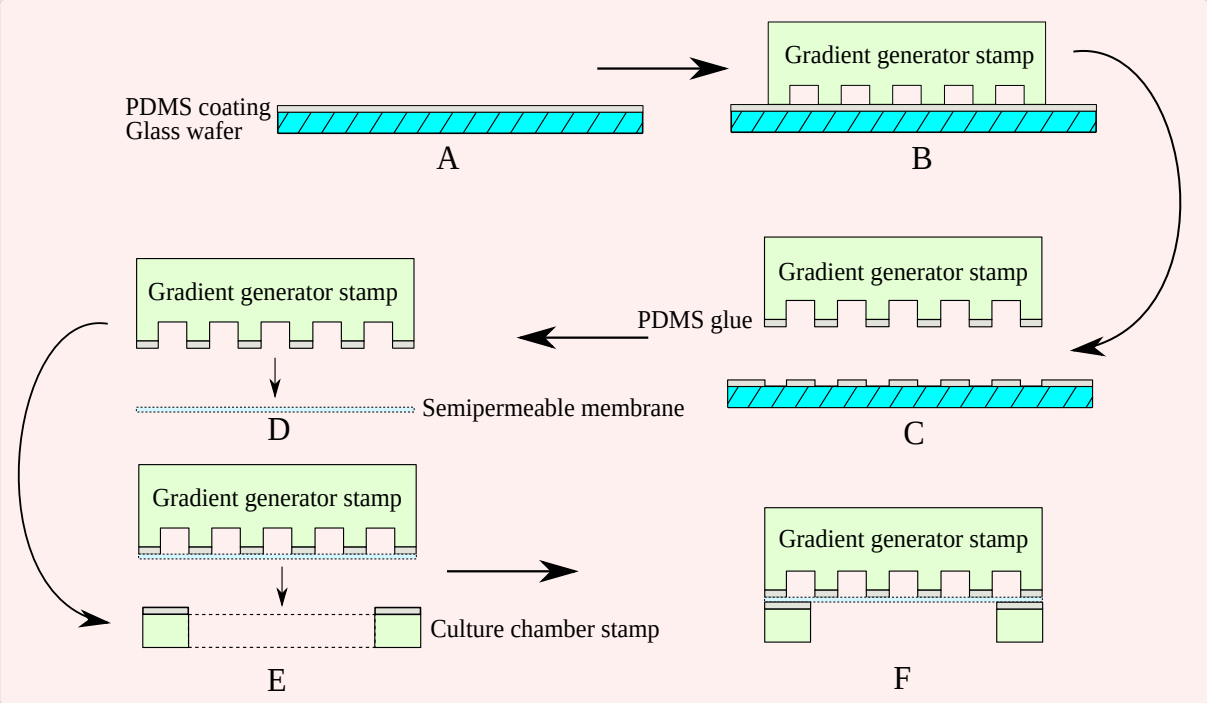

Figure 23: *Bonding of device. A) Thin PDMS layer spun on a glass wafer. B) Gradient generator stamp rolled in a thin layer of PDMS. C) Stamp is released from wafer with a thin PDMS coating serving as glue. D) Semipermeable membrane is bonded to stamp using a pair of tweezers. E) Culture chamber stamp is similarly rolled in uncured PDMS and bonded to the stamp/semipermeable membrane. F) Device is cured in oven to form a strong PDMS bond.*

A second lid similar to the first lid was designed to apply pressure on the edges of the device but to have an opening enabling observation of the channels during experiments.

4.4 Fluorescence Microscopy

An experimental approach to test whether a linear gradient could be generated in the first generation gradient generator was to use fluorescence. Fluorescence intensity increases with an increased concentrations of fluorescent molecules. As fluorescence intensity is not necessarily proportional to the concentration of fluorescent molecules it was necessary to make a standard curve for calibration. In this standard curve, fluorescence intensity is plotted as a function of the concentration of fluorescent molecules and it can be used to determine concentrations generated by the gradient generator. *Fluorescein sodium salt* (fss) was diluted in *Phosphate Buffered Saline* (PBS) in 1:2 dilutions starting from a 1:200 dilution to make a standard series. Following table shows the resulting concentrations, see table 1.

Fss:PBS	1:1	1:200	1:400	1:800	1:1600	1:3200	1:6400	1:12800	1:25600
V_{tot}/ml	10	5	5	5	5	5	5	5	5
$c_{fss}/(mg/l)$	$1*10^5$	500	250	125	62.5	31.25	15.625	7.8125	3.90625
c_{fss}/mM	266.8	1.32	0.664	0.332	0.166	0.083	0.041	0.021	0.010

Table 1: *Generated concentrations of fluorescein sodium salt from 1:2 dilutions. These concentration were used to create the standard curve. The stock solution 1:1 is also included.*

Every dilution was divided into 2 separate syringes (2*2.5 ml), thereby 16 syringes in total. Eight separate experiments were conducted where the fluorescence intensity was determined for every single dilution (concentration) as they were run through the gradient generator. Using ImageJ, an image processing program, it was possible to capture images and collect gray scale intensity values. The procedure for data collection is shown in figure 24. These gray scale values correspond to the fluorescence intensity registered by the camera. To acquire a plot profile showing gray scale values as a function of distance, a straight line was simply drawn according to the figure. This data was then saved as text file and opened in MATLAB where an average gray scale value could be acquired. For every single vertical channel, this measurement was made and average gray scale value was calculated. After calculating the average gray scale value for every vertical channel in the gradient generator, a total average gray scale value was calculated from these values. The total average gray scale value for every dilution was plotted and a curve was fitted and used as the standard curve.

To evaluate whether the gradient generator could generate a linear gradient, the dilution 1:200(100% fss) was injected into one inlet while PBS(0% fss) was injected into the other inlet. After taking images of all channels and analyzing them using ImageJ, the measured intensities were used with the standard curve to aquire the specific concentrations in each channel. The gradient profile could then be plotted in MATLAB.

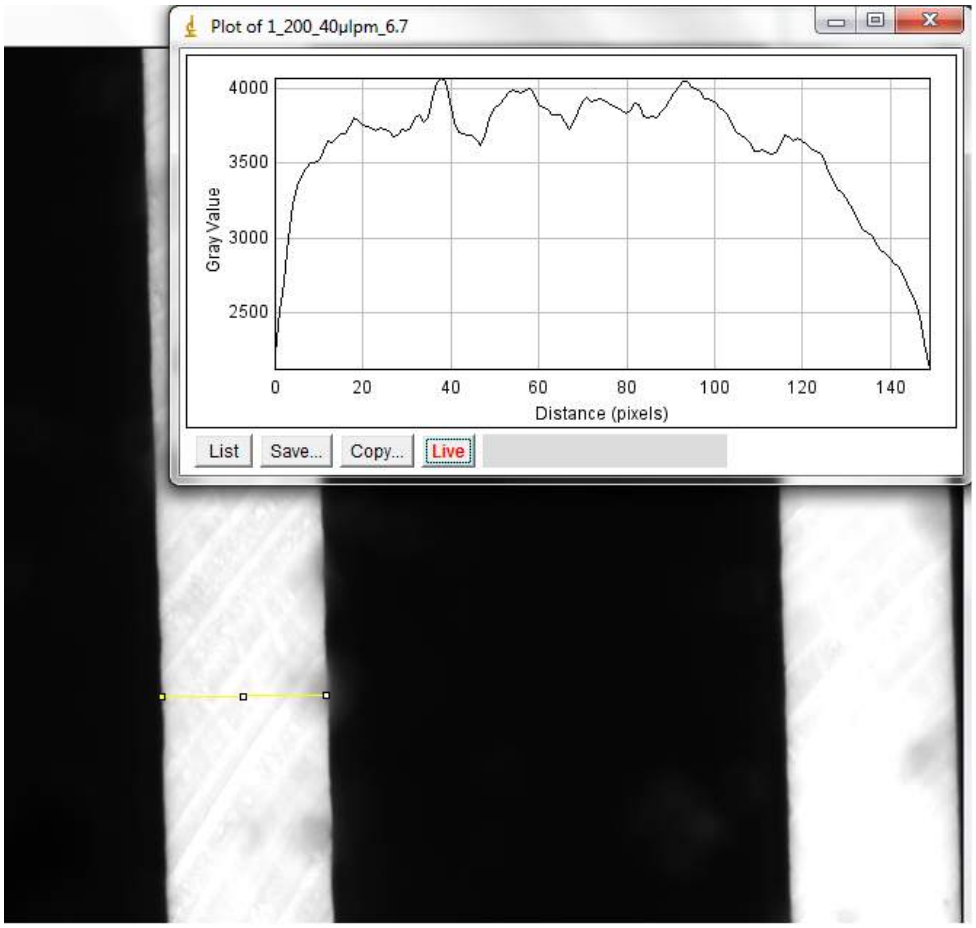

Figure 24: *Gray scale image taken of the vertical gradient channels. The same concentration, 1:200, is run through all channels. Intensity values are acquired by drawing a yellow horizontal line across each of the channels, in this case the left channel, and then plot the result. For every experiment the same magnification was used.*

4.5 Differentiation of human embryonic stem cells

4.5.1 Priming of the system

Before starting a differentiation experiment it was necessary to eliminate bubbles in the gradient channels that could affect the gradient formation and the cells in the culture chamber. Therefore the microfluidic system had to be run for 24 hours in order to prime it. The microfluidic device was initially immersed in ethanol 70 (v/v)% as contamination might affect cell viability. Four syringes(10 ml, BD Plastic) were filled with cell medium having the dissolved GSK3i concentrations: $6\mu M(100\%)$, $3\mu M$, $3\mu M(50\%)$ and $0\mu M(0\%)$. Long teflon tubings were connected between the syringes and the inlets of the device and between the waste container and the outlets of the device, as shown in the figure 25a. After connecting the syringes, the microfluidic device was immersed a cell culture dish with only cell medium. To avoid trapping air in the culture chamber the device had to be sligthly slanted when immersing it. The device was then mounted in the device holder using eight screws and nuts to ensure proper contact between the bottom of the petri dish and the device. The holder/device assembly was then placed inside an incubator having a temperature of 37°C. Syringes were mounted in the syringe pumps outside the incubator. The two pumps supplying the gradient generator with cell medium

were set to have a flow of 40 $\mu l/h$. The third pump supplying the culture chamber with cell medium were set to have a flow rate of 160 $\mu l/h$. It was also placed on an elevation of 30 cm to exert a hydrostatic pressure in the culture chamber to collapse bubbles. The waste container was placed on the same elevation. All pumps were then started to run for 24 hours.

4.5.2 Differentiation of hESCs: placing the device on the cells

After 24 hours, the pumps were switched off and the device was immersed into another cell culture dish with fixed hESCs at the bottom, see figure 25b. The device was then mounted again in the device holder and inserted into the incubator. Pumps were started to supply cells with medium and initiate differentiation. The experiment would run for 9 days for hESCs to differentiate into cells of forebrain, midbrain and hindbrain.

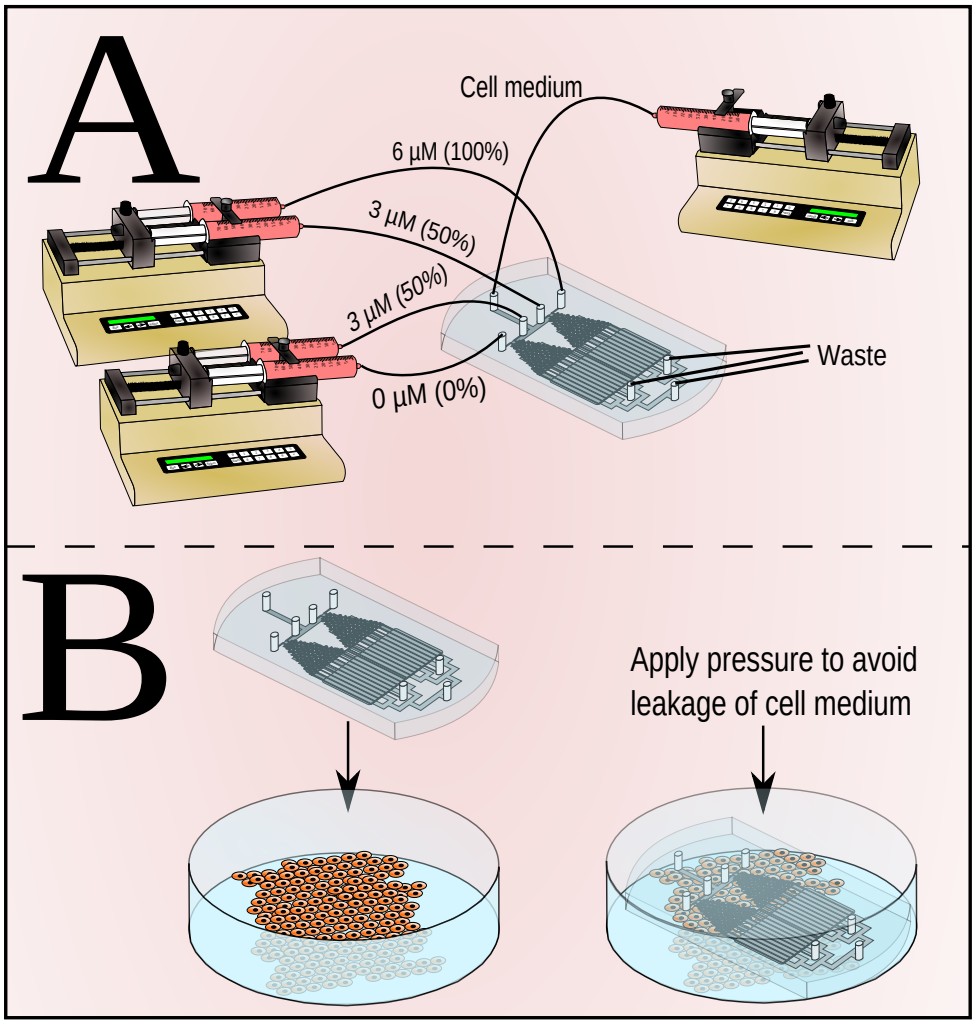

Figure 25: *Part of experimental setup. A) Connection of pumps to the inlets of the microfluidic device. B) Immersion of microfluidic device on hESCs at the bottom of the cell culture dish. By using the device holder, a pressure was applied on the device to fix it in the cell culture dish and to aviod leakage of cell medium.*

5 Results

5.1 Simulations in 2D

5.1.1 Gradient profiles

First generation gradient generator

A simulation of the first generation gradient generator, used initially in the project, is seen in figure 26a. When plotting the average concentrations for each vertical channel the gradient had a step-like profile, seen in figure 26b. No linear gradient could be generated even if the diffusion coefficient was varied and the flow speed was decreased to achieve complete mixing in the mixing channels. A finer mesh was not used and not necessary as the given solution using the normal mesh clearly illustrated the gradient formation.

Second generation gradient generator

The same simulations were performed for the second generation gradient generator, see figure 27. A linear gradient could be generated. Therefore, it was decided to continue with this design for fabrication instead of the first gradient generator.

5.1.2 Flow in culture chamber

The two dimensional simulation of the velocity magnitude in the culture chamber resulted in the following surface plot, see figure 28a. When plotting the velocity along the 2 cm wide culture chamber, a rather parabolic velocity magnitude profile could be seen, see figure 28b. The average flow velocity and the median velocity are indicated in the figure. A theoretical value was calculated to evaluate the plausibility of these values and it was found to be in between the median velocity and the average velocity. As the theoretical value was close to these values, the simulation seemed plausible.

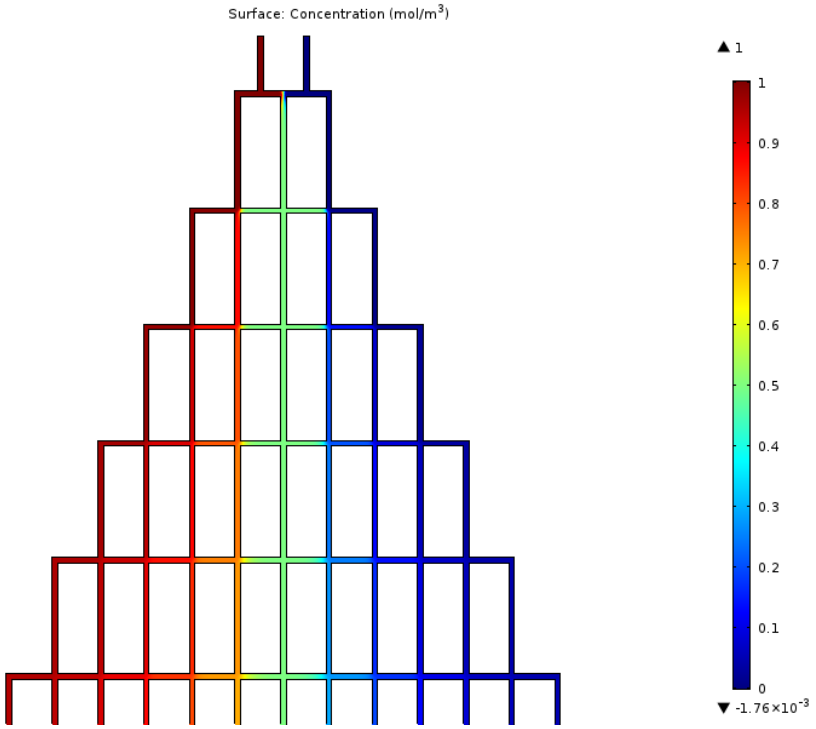

(a) *Concentrations generated in the first gradient generator. Each color represents a specific concentration, seen in the color bar.*

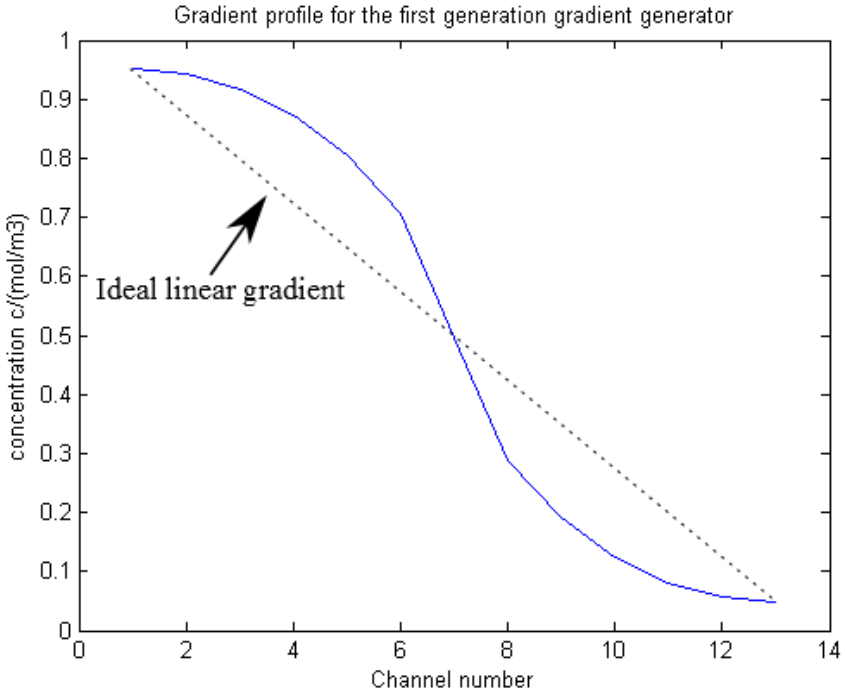

(b) *Concentration gradient for the first gradient generator. Concentrations vary considerably between the middle channels in comparison to the outer channels where the concentration values are more adjacent. It results in a more sharp step-like gradient profile rather than a linear gradient indicated by the black dotted line.*

Figure 26: *Simulation of the first generation gradient generator.*

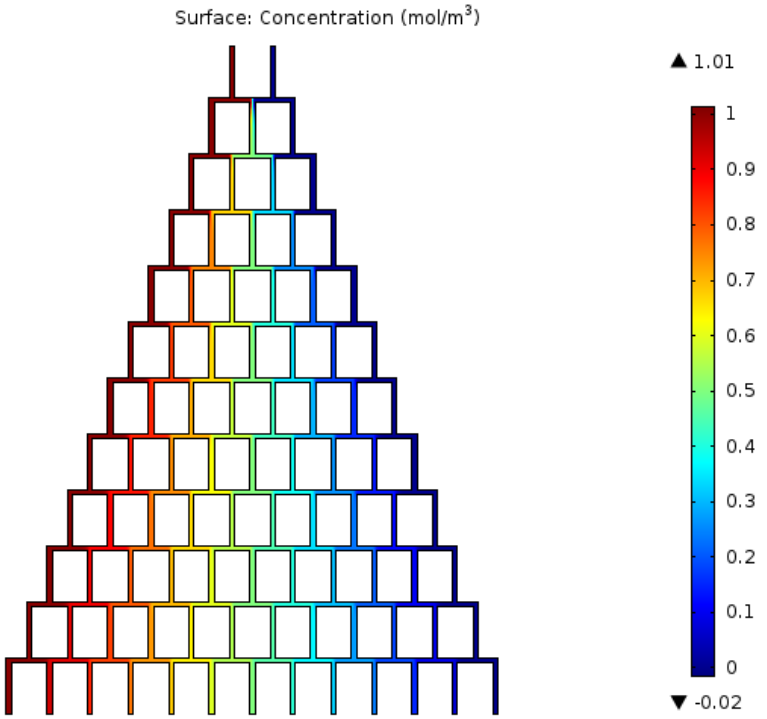

(a) *Concentration surface plot of second generation gradient generator.*

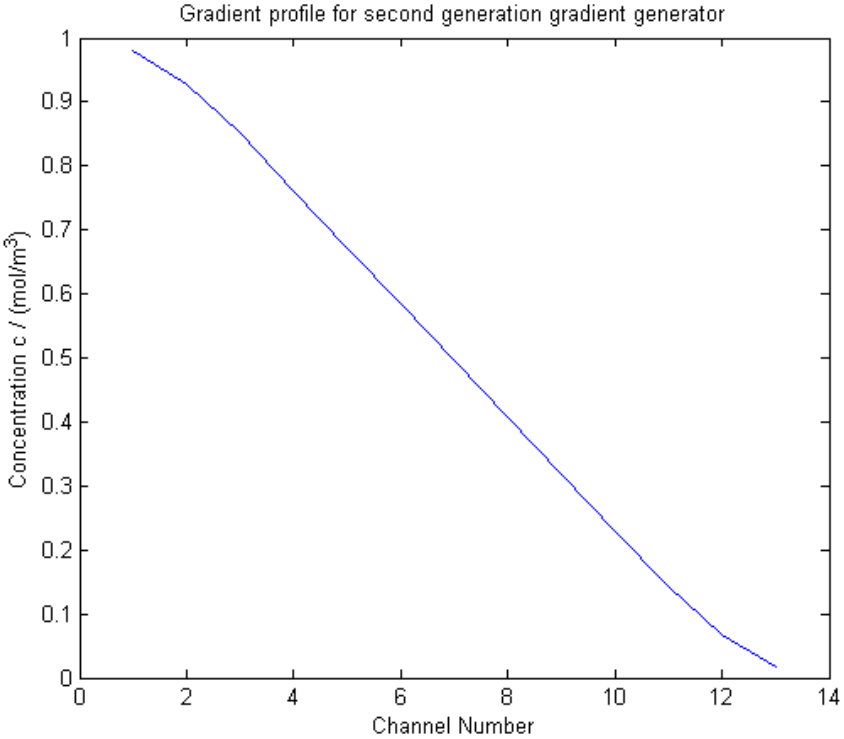

(b) *Gradient profile for the second generation gradient generator. A linear gradient profile is generated.*

Figure 27: *Simulation of the second generation gradient generator*

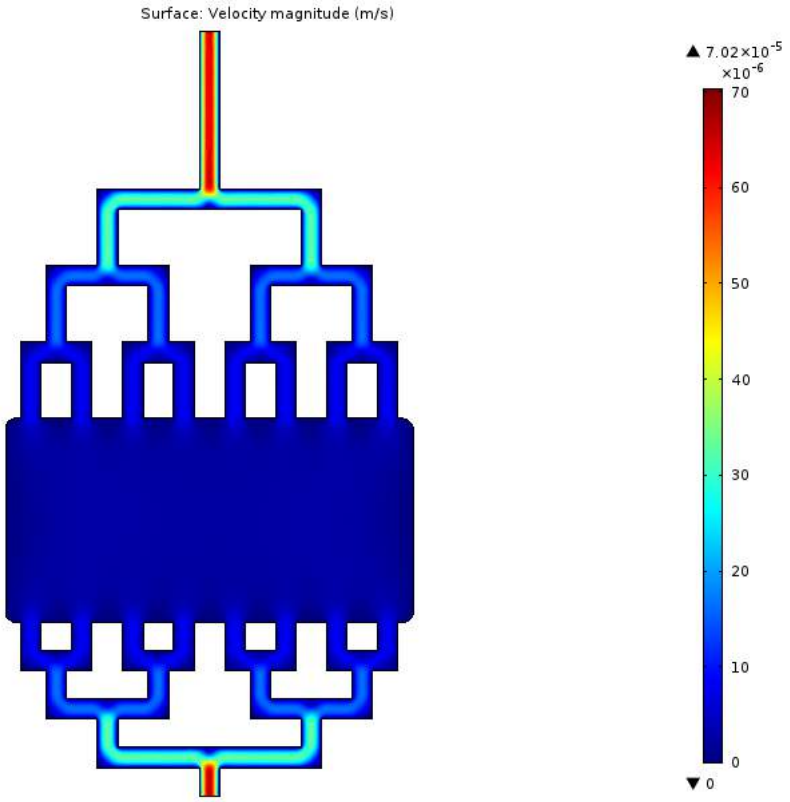

(a) *Surface plot showing the velocity magnitude in the culture chamber.*

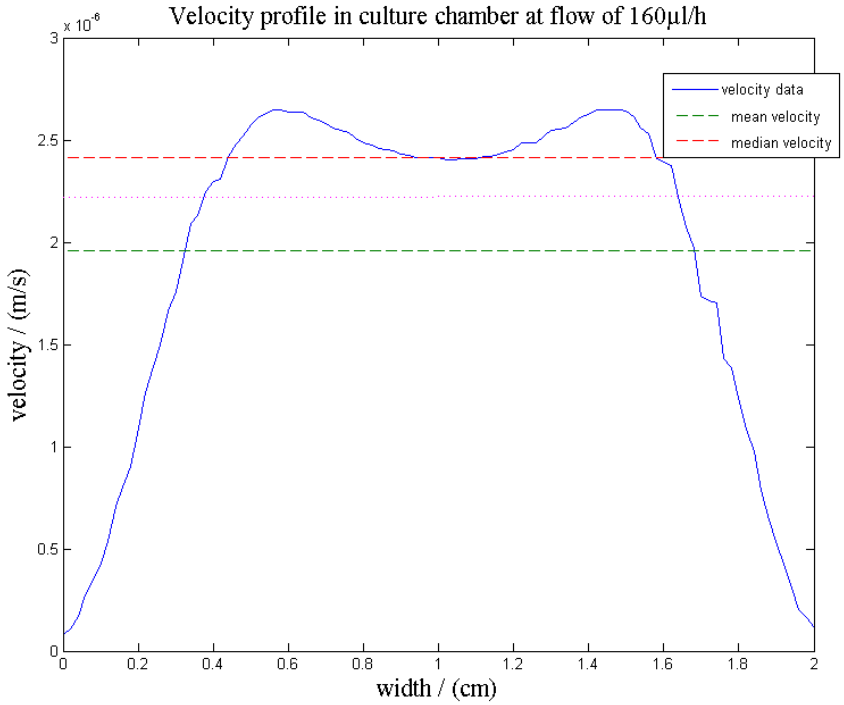

(b) *Velocity magnitude profile for the culture chamber. The mean velocity is indicated by the red line while the median velocity is indicated by the dark green line. A theoretical value for the mean velocity magnitude is given by the dotted pink line in between the two other straight lines.*

Figure 28: *Culture chamber simulation.*

5.2 Fabrication of microfluidic system

5.2.1 Gradient generator fabrication

Masters were initially fabricated on both silicon and glass, see figure 29.

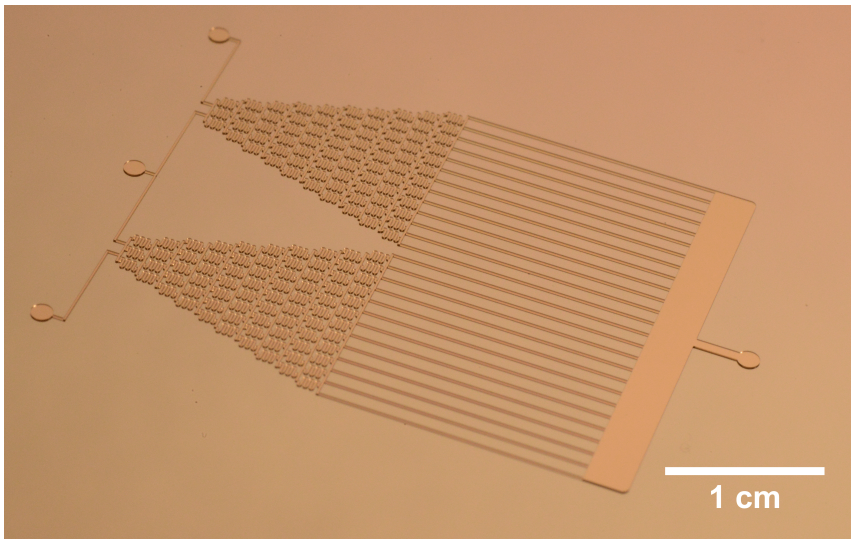

(a) *Silicon master with gradient generator design A.*

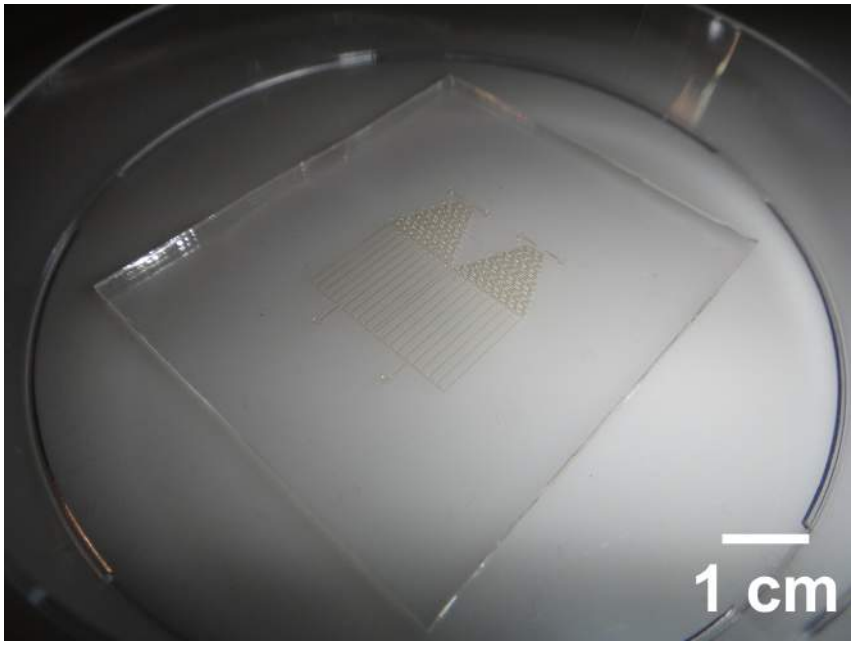

(b) *Glass master with gradient generator design D.*

Figure 29: *Masters fabricated in a clean room. The mask patterns have been accurately transferred to the resist after development.*

Due to the brittle nature of silicon, a master fabricated on such a substrate would easily break when reusing it more than once. It was therefore decided to make all subsequent masters on a glass substrate.

5.2.2 Gradient generator stamp

The first attempts to create PDMS stamps from fabricated glass masters were problematic. Small molded features in a stamp were easily torn when manually peeling off the stamp from the master, see figure 30.

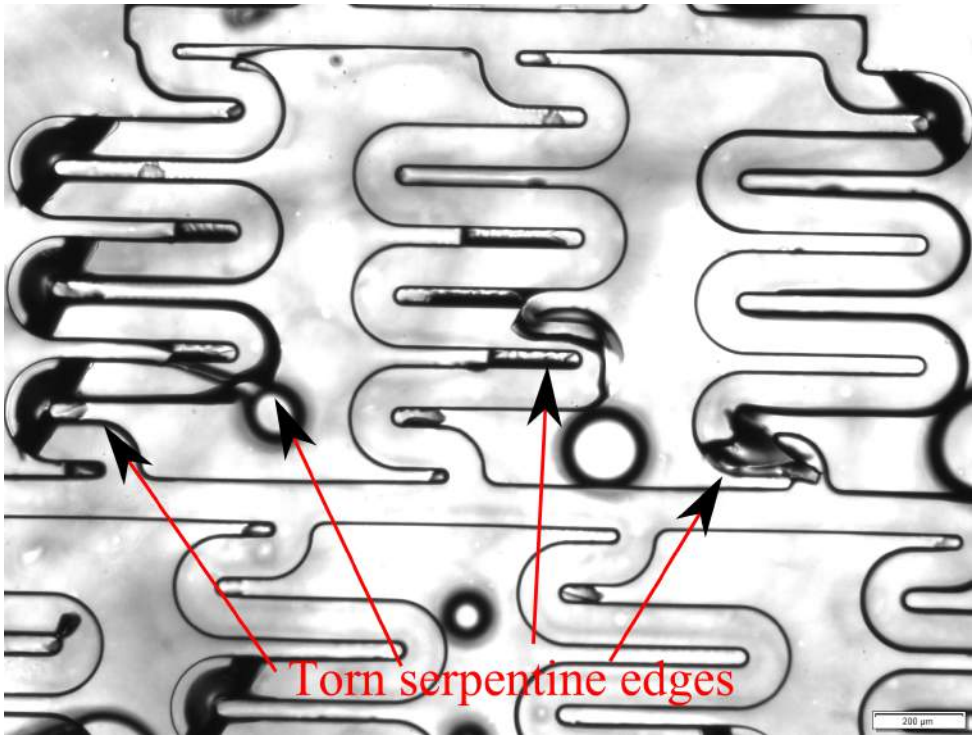

Figure 30: *PDMS details are torn at the edges of the serpentine channels after peel off. In this case the PDMS stamp is fabricated from design A.*

These broken stamps were not used for later bonding or experiments.

This problem was solved when the master was coated with PVA, prior to molding with PDMS. It was then possible to peel off the stamp without tearing any structures.

5.2.3 Assembly of microfluidic system

It was possible to assemble a device using PDMS as glue with the gradient generator stamp having design D. The device was properly sealed after curing of the PDMS glue and the membrane was bonded to the gradient channels.

An attempt to bond a gradient generator stamp with design A was performed. However after assembling the device, uncured PDMS could be seen to enter the channels and even clog some vertical channels in the gradient generator stamp. It was decided to not continue with design A for future bonding events, see figure 31.

5.3 Device holder fabrication

One bottom piece was created with a milled central cavity tailored for partly submerging a 60 mm cell culture dish. Eight holes were evenly milled in the bottom piece to enable

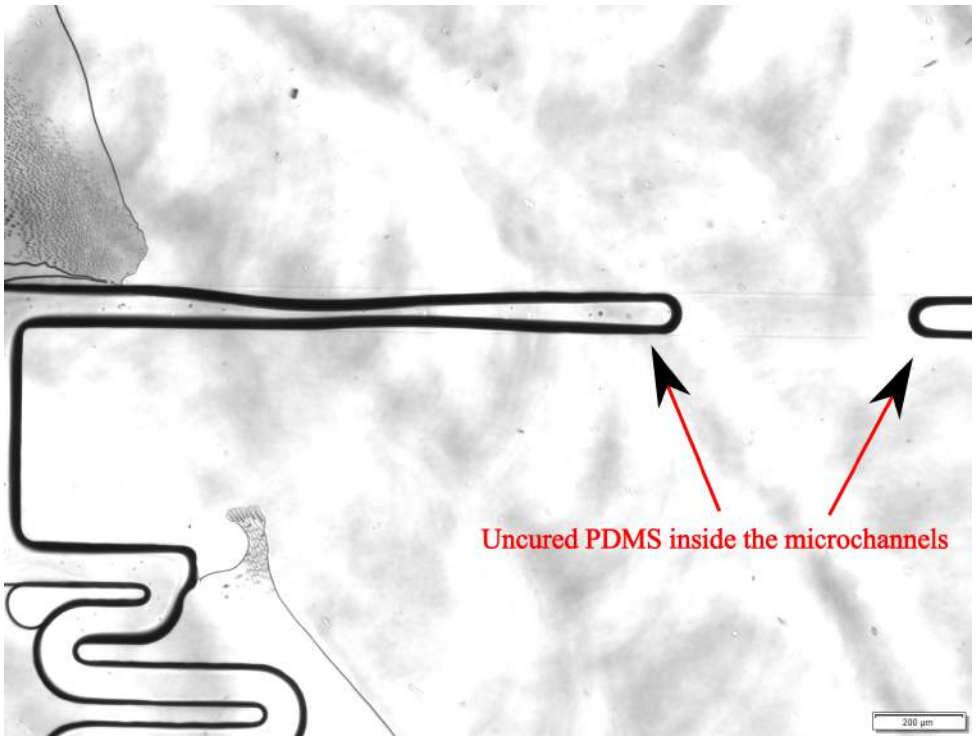

Figure 31: *Part of a gradient generator stamp with design A. Uncured PDMS has entered the right inlet channel indicated by the arrows.*

attachment of a lid piece, see figure 32.

The first fabricated lid piece had milled holes for inlets and outlets of the device. It could thereby apply an even pressure on the microfluidic device situated in a cell culture dish when mounting it with eight screws and nuts.

The second lid got a shape similar to the first lid but it had a small opening in the middle to allow for observation of the device during experiments. Pressure could still be applied around the edges of the device to prevent leakage of cell medium from the culture chamber, see figure 33.

Figure 32: *Bottom piece of the device holder. A cell culture dish is submerged into the milled cavity. Eight screw holes are evenly milled around the cell culture dish.*

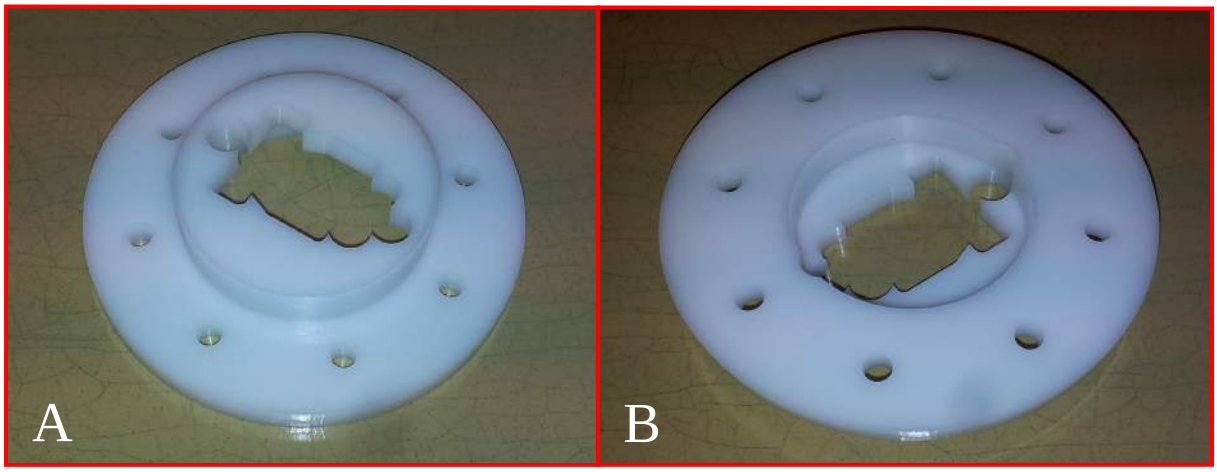

Figure 33: *A) Bottom view of lid. It is an opening in the middle for observing the device during experiments. The middle is elevated to apply a pressure on the device located in the cell culture dish. B) Top view of lid.*

5.4 Culture chamber fabrication

A first culture chamber PDMS mold was designed in Galaad having the dimensions seen in figure 18. The area of the rectangular culture chamber part was 2*1 cm^2 and it was made using both a 3 mm and a 1 mm diameter cutting tool. After the milling procedure, most edges and surfaces were rough due to the fact that the cutting tools were worn out from previous millings. After an ultrasonic bath, many plastic residues could be removed from the bottom piece and the edges were less rough which could be felt by a finger and with a scalpel blade. It was decided to not use this bottom piece for injection molding since surfaces still were rough after ultrasonic bath. Also, a 2 cm wide culture chamber

would require perfect alignment with a gradient generator during bonding since the vertical channel region of gradient generator design D is 2 cm wide.

Another culture chamber bottom piece was therefore fabricated. The width of the culture chamber part was increased to 2.2 cm to allow for some misalignments while other dimensions were kept the same. New cutting tools were used which resulted in smooth edges and surfaces. Inlet and outlet markings were also milled out in the bottom piece which would facilitate creating inlet and outlet holes in the PDMS stamp. This bottom piece was later used for injection molding.

5.5 Fluorescence Microscopy

5.5.1 Determination of concentrations in the first generation gradient generator

The standard curve for fluorescein sodium salt diluted PBS is seen in figure 34. Following

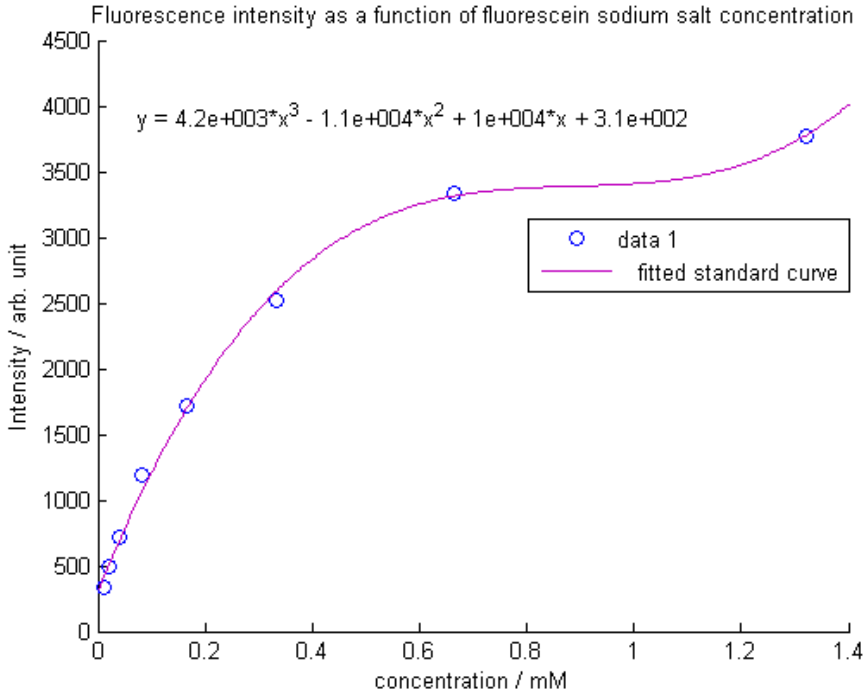

Figure 34: *Standard curve fitted to eight fluorescence intensity values measured for specific concentrations of fluorescein sodium salt. The dots represents the intensity values determined from the dilutions in table 1.*

average intensities were measured for 11 out of 13 channels in total when injecting the 1:200 (100% fss) into the first inlet and pure PBS (0% fss) into the second inlet, see table 2.

Intensity/arb. units	N/A	805	1075	1480	2019	2699	3451	3577	3686	3492	3584	3398	N/A
Conc./mM	N/A	0.05	0.08	0.14	0.22	0.37	0.87	1.08	1.18	0.97	1.09	0.76	N/A
Channel Number	1	2	3	4	5	6	7	8	9	10	11	12	13

Table 2: *Acquired fluorescence intensity values from the gradient experiment. Concentrations could be deduced from the standard curve, see figure 34.*

Corresponding concentration value for every intensity value listed in table 2 was determined using the standard curve. These values were then plotted in figure 35. As seen in the figure, from channel 10-12 the concentrations are lower than in channel 9 which is unexpected. Reasons for this deviation will be reviewed in the discussion. A step-like profile is however expected for the first generation gradient generator.

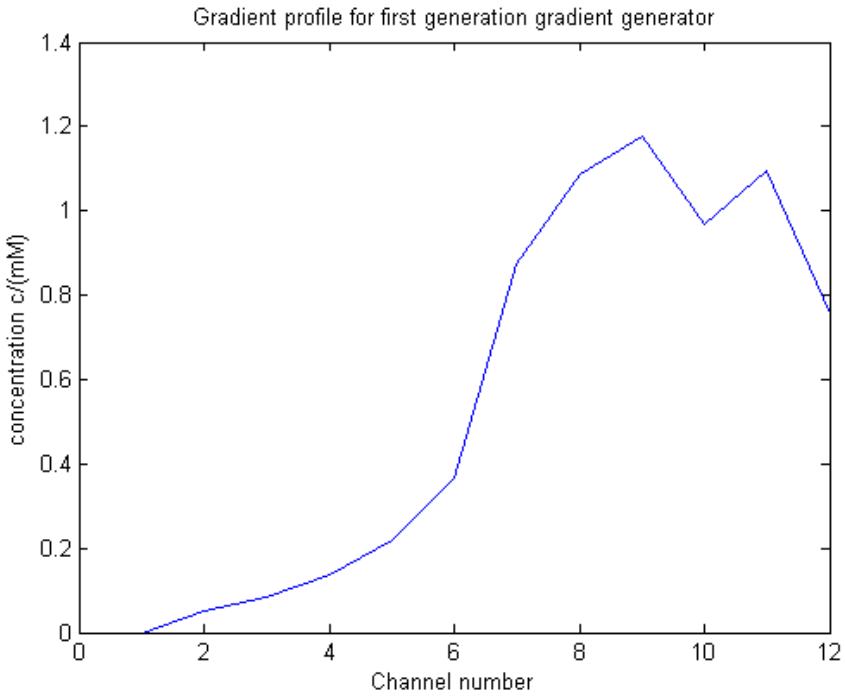

Figure 35: *Gradient profile for the first generation gradient generator. It has a step-like profile as expected.*

5.5.2 Qualitative determination of gradientprofile in the second generation gradient generator.

Two different profiles were generated in the second generation gradient generator. When using a higher flow rate of 100 μl/min the transition between channel 5 and 6 was very sharp seen by the difference in intensity. It indicates a more step-like gradient profile, as shown in figure 36a. But when the flow rate was set to 40 μl/h a more linear gradient could be generated. It is represented by the small difference in concentration between the middle channels, see figure 36.

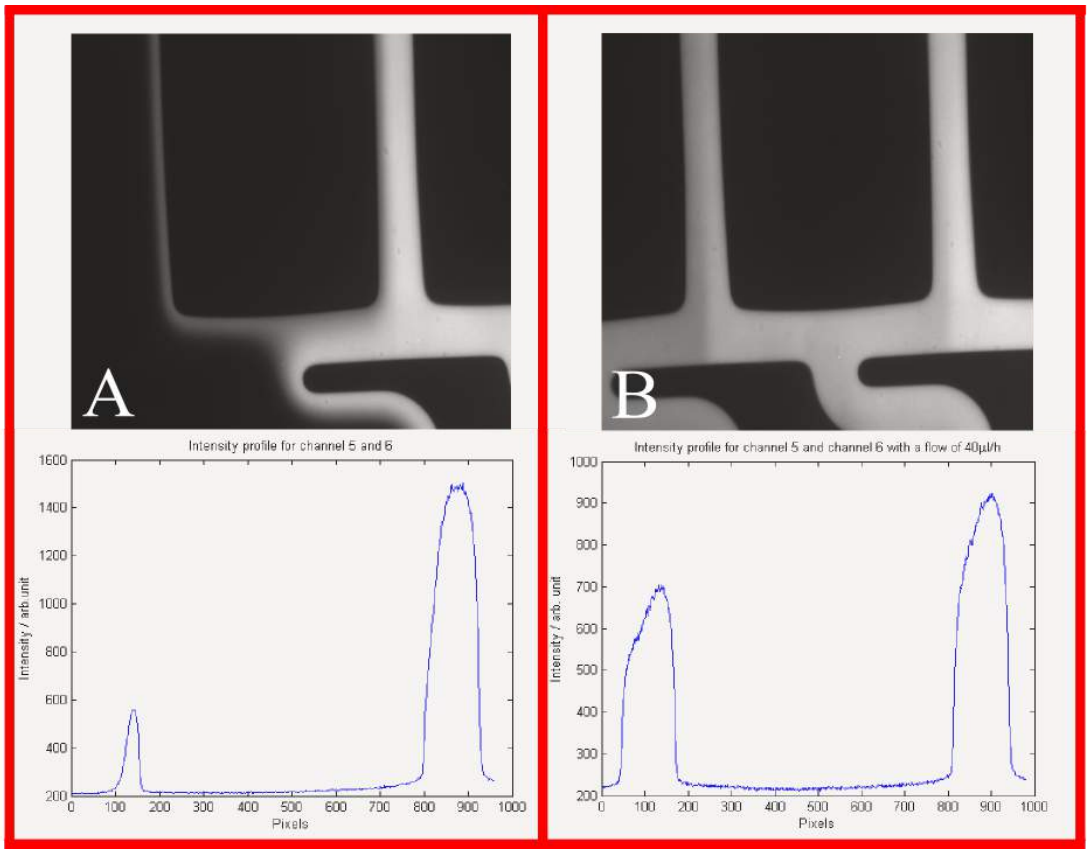

Figure 36: *A) Steep transition between concentrations where the concentration of fluorescein sodium salt in channel 5 is very low in comparison to channel 6 with a flow rate of 100 µl/min. B) Small difference in concentration between channel 5 and 6 as indicated by the small difference in intensity with a flow rate of 40 µl/h. The intensity profiles are plotted for both cases.*

5.6 Differentiation of hESCs

5.6.1 Experiment

After priming the system for 24 hours no bubbles were visible in the culture chamber or the gradient channels. It was therefore possible to transfer the microfluidic system to a new culture dish with hESCs to initiate a differentiation experiment, given that no bubbles would be introduced during the transfer. Pumps would run for 9 days without any interference except for control of bubble formation or leakage of cell medium from the culture chamber. At the end of an experiment, it was possible to observe a color change in the culture chamber from the natural pink color to a more yellow color. It was an indication that the cells were proliferating, see figure 37. After 9 days, the microfluidic system was demounted from the cell culture dish and cells could be observed in the culture chamber, see figure 38. Cells were collected from the 5 regions in the cell culture dish denoted A-F. Each region was then divided into 2 fractions (FIX and RNA) as seen in the figure.

5.6.2 Qualitative and quantitative analysis

Cells collected from the fix fractions were analyzed qualitatively in order to investigate whether there was any difference in phenotype between fraction A and fraction E. A forebrain and midbrain phenotype was found in fix fraction A-D as the forebrain-midbrain genetic markers, OTX2 and LMX1A, were expressed, see figure 39. Antibodies specific for OTX2 had a red fluorescent dye molecule linked while antibodies specific for LMX1A had a green fluorescent dye linked to them as seen in the figure. No forebrain-midbrain cells were detected in region E-F as there was basically no fluorescent signal from antibodies specific for OTX2 and LMX1A. No suitable antibodies were available in order to detect a hindbrain phenotype in fixed fraction E-F. A background control using the fluorescent dye *4',6-diamidino-2-phenylindole*(DAPI) was performed to verify whether cells were present in all fractions prior to the fixed cell analysis. As seen in figure 39, there are cells in all fixed fractions.

A real-time polymerase chain reaction assay (qRT-PCR) was performed after the fixed analysis to more quantitatively understand how successful the differentiation had been. For the qRT-PCR assay, cells were collected from the RNA fractions A-E, see figure 38. The gene expression level for 6 genes expressed in forebrain, midbrain and hindbrain respectively were analyzed for each fraction A-E. The gene expression level for each fraction was then normalized with respect to the maximum value of gene expression, see figure 40. Forebrain genes FOXG1 and NKX.2.2 were predominantly expressed in RNA fraction A and B. Midbrain genes LMX1A, EN1 and WNT1 had a maximum gene expression level in RNA fraction C while hindbrain genes HOXA2 and NKX6.1 were abundantly expressed in RNA fraction D and E.

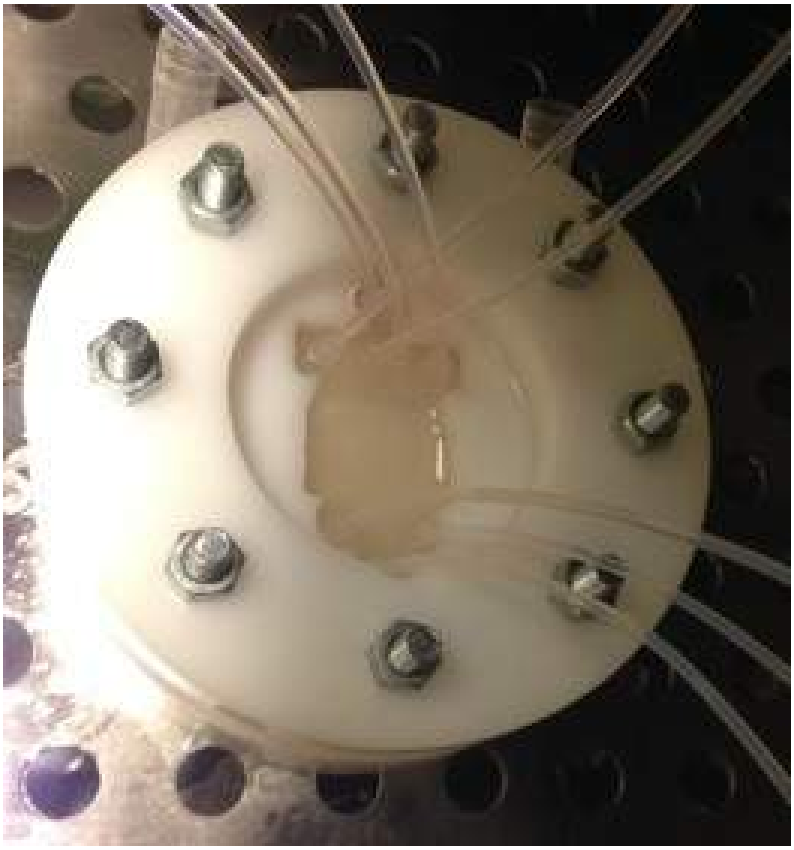

Figure 37: *Top view of the device during the third experiment. The medium has changed color from pink to a more white-yellow color in the culture chamber, indicating that cells are proliferating.*

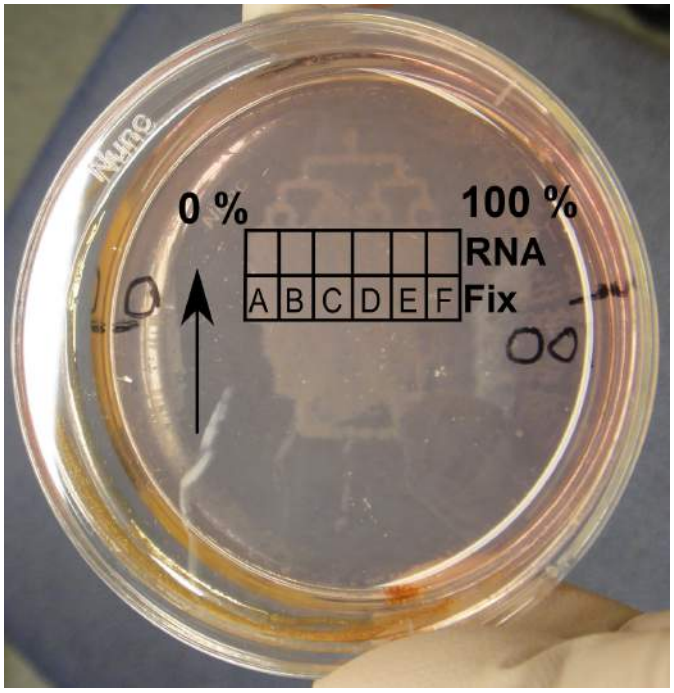

Figure 38: *Cells are visible in the cell culture dish after 9 days culturing. They have taken the shape of the cell culture chamber. Cells were divided into five regions, A-E where they could be collected for fixed analysis and qRT-PCR.*

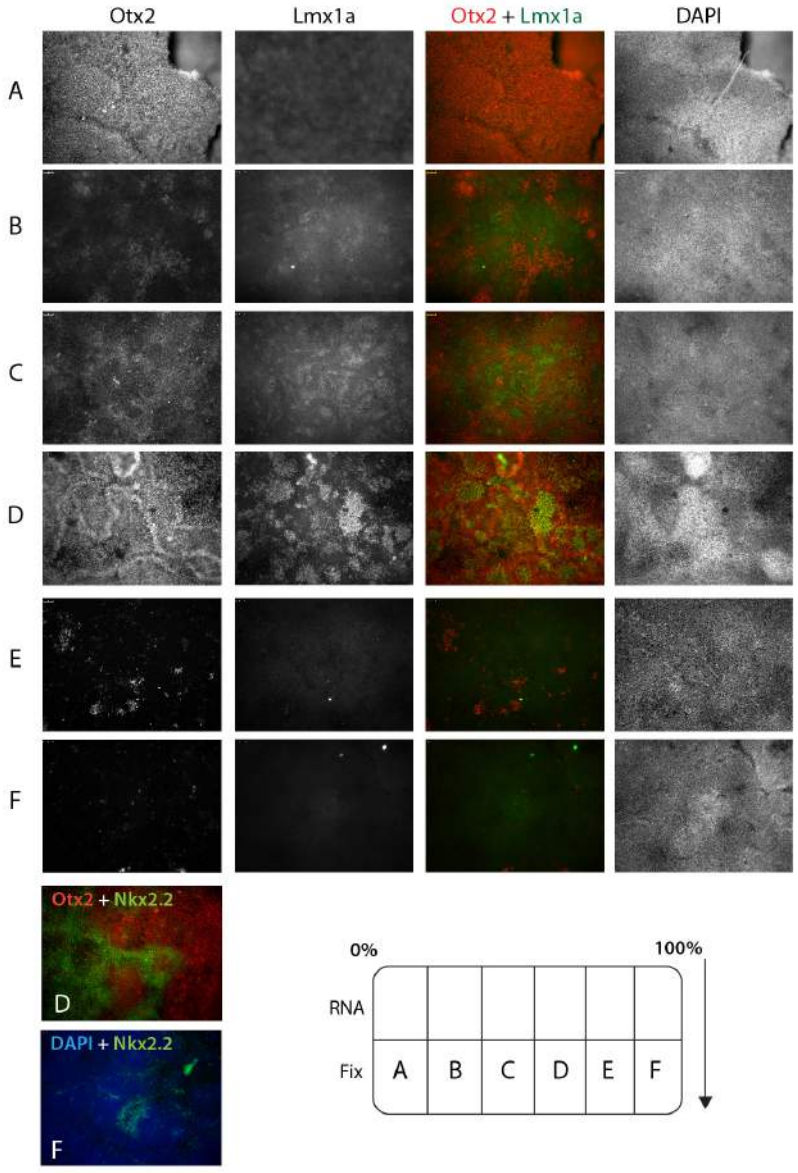

Figure 39: *Cells in the fixed region are collected and identified using specific antibodies. Forebrain and midbrain cells are identified in fixed fraction A-D. As OTX2 and LMX1A are genes that are not expressed in hindbrain cells, it indicates that these cells are found in fixed fraction E-F. It is confirmed by observing region E and F, as there is basically no fluorescent signal for OTX2 and LMX1A. DAPI serves as a fluorescent background control to ensure that cells are present in all fixed fractions.*

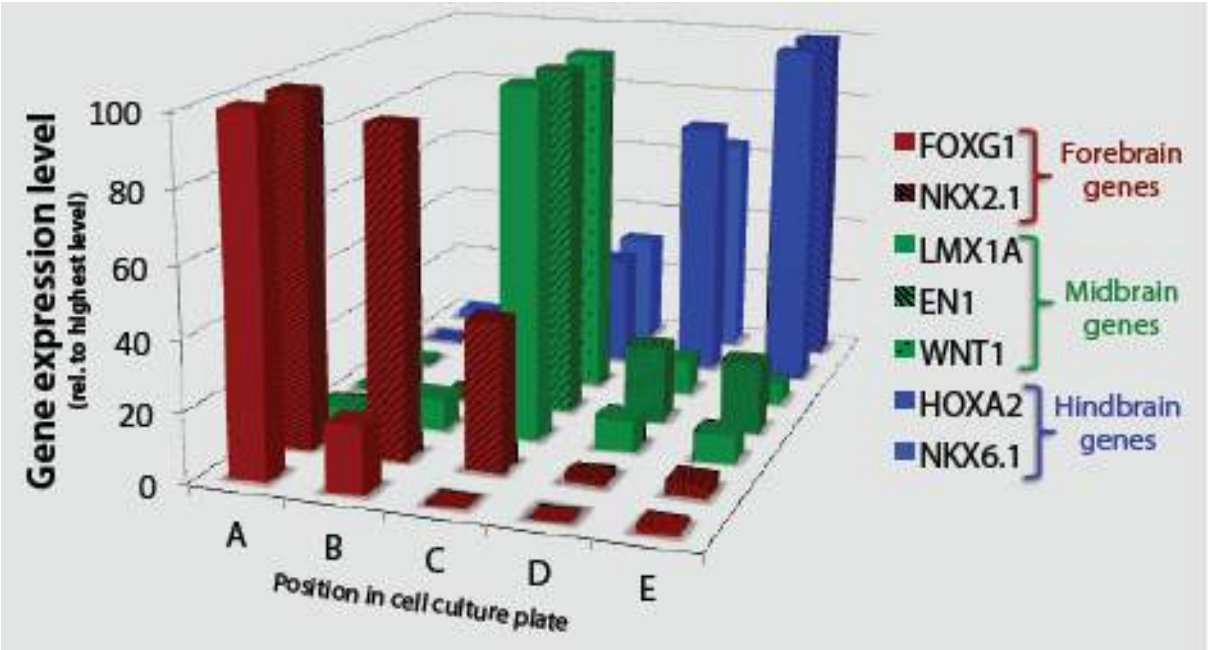

Figure 40: *Bar plot visualising the gene expression level for 6 different genes expressed in forebrain, midbrain and hindbrain in the different RNA fractions A-E. These fractions can be identified by observing figure 38.*

6 Discussion

Soft lithography allows for simplifications regarding fabrication of microchannels. A microfluidic device can be fabricated in less than one day, including the fabrication time for the master. Using PDMS as material also has several advantages in terms of robustness and biocompatibility. However, the master fabrication process can be rather problematic due to several reasons. Creating a master involves several manual handling steps where the master could be destroyed or defect. Firstly, avoiding bubble formation in the resist before spinning can be difficult when withdrawing resist from the glass container using a Pasteur pipette. If bubbles are small it is sometimes hard to pop them using a sharp tweezer. Small cavities are also formed after popping the bubbles making the resist uneven at certain places. When having a fabricated master, the PVA treatment is essential for succeeding in the process of peeling off the PDMS stamp. PVA forms a rather thin and homogeneous layer but it tends to accumulate at the edges of the channels affecting the geometry in some places as seen in figure 20b. Even if PVA is water soluble, it can be difficult removing undissolved PVA from the master. After molding a master for more than five times, the master could be greasy resulting in disposal of the master. Since the resist has a varied thickness on the wafer the channels will have a varied thickness. Assembly of the microfluidic device can be performed in less than 1 hour but some bonding steps are difficult and very critical. Attaching the semipermeable membrane is especially difficult since the membrane has a very light mass and thereby flickers much in the presence of any air streams. In a clean room facility where there is a considerable ventilation of the air, makes it difficult to attach and align the membrane. Some air could also be trapped in between the membrane and the gradient generator stamp preventing sufficient bonding. The membrane also constitutes the weakest point of the device since it easily detaches from the gradient generator stamp when flushing out bubbles from the gradient channels prior to experiments. It was the reason for priming the system for 24 hours as bubbles would collapse due to the hydrostatic pressure, removing the need to flush out bubbles.

Both device holder lids have their advantages and their disadvantages. The first lid has the advantage of applying an even pressure on the entire device. But since it is non-transparent it is not possible to observe the culture chamber during experiments for detection of bubbles or breakage of membrane. Therefore another open lid was made that would apply pressure on the edges of the culture chamber and allow for observation during experiments. By seeing the cell culture in figure 38, it is seen that cells have been growing between the channels. It means that the PDMS has not been in proper contact with the bottom of the cell culture dish.

The first device created at the origin of this project made use of the gradient generator design seen in figure 26a. It is a simplified design which was possible to create using the milling machine. However, two dimensional simulations made in COMSOL suggest that it is not possible to create a linear gradient even if concentration equilibrium prevails at the end of every mixing channel. Therefore, it was decided to not proceed with this design but with a new gradient generator design having serpentine channels and T-junctions. Regarding the flow profile in the culture chamber, it is not as homogeneous as expected. A parabolic flow profile is always present when the flow is laminar but a more flattened profile would be desirable. In order to fully understand the flow in the culture chamber, a 3D simulation could be necessary with the correct parameters.

Even if simulations above are essential for understanding the flows in the device, one important simulation remains. It serves to answer the question: How does diffusion affect the linear gradient in the culture chamber? GSK3i molecules have to diffuse a distance of 1mm from the vertical gradient channels to the bottom of the petri dish where cells are located. Since diffusion is isotropic, there will also be horizontal diffusion and as a consequence of Ficks first law, the linear concentration gradient will in time be equalized. In order to avoid concentration equilibrium in the culture chamber, it is necessary to understand the relation between diffusion and convection as given by the Péclet number. A 3D simulation of the diffusional transport between the gradient channels and the cells is thus essential for optimization of the device.

Since fluorescence intensity increases with increased concentration, fluorescence microscopy is a means of visualizing different gradient profiles and determine concentrations. Generating different gradient profiles is possible by simply varying the flow rates. When having a flow rate of 100 μl/min at each inlet there is not sufficient time for diffusional mixing in the serpentine channels. It results in a more step-like gradient profile. Since all gradient channels could not be visualized in the camera, images of the middle channels 5 and 6 were taken. When making a significant decrease in flow rate, to 40 μl/h there is time for diffusional mixing in the serpentine channels resulting in a smoother and more linear gradient profile. A more scientific explanation involves the different Péclet numbers. For 100 μl/min, the Péclet number has a higher magnitude than for 40 μl/h. For a lower Péclet number there is more diffusional transport in relation to convectional transport.

Using fluorescence to determine specific concentrations is a more complicated process. First a standard series needs to be created which is time consuming especially as all concentrations have to be run through the gradient generator and images had to be taken of every vertical channel. Even if the gradient profile in figure 35 is expected some channels are deviating considerably. A defect was found preventing fluid flow in the outer gradient channels when observing the gradient generator stamp. This might have been the cause for the deviating results. Using the the standard curve in figure 34 is not suitable if the measured fluorescence intensities are in the plateau region. Judging from table 2, the determined concentrations in channels 7-12 are based on intensity measurements in the plateau region. These concentrations are therefore rather uncertain as background noise could lead to measurement errors and incorrect results. If more time was available for this part it would be necessary to make a standard series from dilutions having intensities in the linear region in figure 34 along with a better curve fitting. Also, it could be necessary to eliminate fluorescent noise from PDMS as it is autofluorescent.

A less time-consuming way and more accurate method to use fluorescence would be to use a plate reader with the different dilutions in separate Eppendorf tubes to create a standard series. Then a gradient generator with the ability to sample the different concentrations in new Eppendorf tubes would allow for determination of fluorescein sodium salt concentrations. However, it was not possible to perform this experiment due to time restrictions.

Many of the earliest experiments resulted in having a broken device or dead cells due to bubbles. Reaching the point of having a flawless experiment without any dead cells and completing the preparations has been problematic. Bubbles would nucleate and grow inside the culture chamber even if no bubbles were present from the start. A first thought

was to degas the cell medium but it would not work since cells need dissolved oxygen and carbon dioxide. After a couple of experiments resulting in dead cells due to bubbles, an article [21], was found providing tips for avoiding bubble formation in a perfusion cell culture system. By simply placing waste and pumps high relative to the microfluidic system, bubbles arising in the culture chamber would collapse. Ever since this setup was used, no bubbles have been present in the culture chamber.

Cells in the fixed fractions A-E were collected and analyzed using specific antibodies. Even if a forebrain-midbrain phenotype was found in A-D, this method is not sufficient to evaluate the success of the differentiation. Genetic marker OTX2 is expressed in both forebrain and midbrain cells and it can thus not be used to determine the difference between these cells. Therefore, it would have been necessary to use antibodies specific for genetic marker FOXG1 which is solely expressed in forebrain cells but they were not available in time of the analysis. There were also no suitable antibodies for detecting the hindbrain cells in region E and F. But when studying figure 39 no antibodies specific for OTX2 are bound to cells in region E-F. Since hindbrain cells do not express OTX2 the exclusion principle indicates that hindbrain cells are present in these two regions. Even if the analysis with the fixed cells can ascertain a phenotype change from fixed fraction A-F, this analysis cannot be used to discover neural subtypes within the three cerebral vesicles. It was therefore necessary to perform a qRT-PCR analysis to look at several genetic markers and their gene expression where the most important where plotted in fig 40. The figure clearly shows a forebrain phenotype in RNA fraction A-B, a midbrain phenotype in fraction C and a hindbrain phenotype in fraction D-E.

7 Conclusions and future aspects

Simulations of two different gradient generator designs were performed in 2D using COMSOL to understand if it was possible simulate the gradient formation and also plot the final gradient profile. The surface plots and the plot diagrams in figure 26 and figure 27 show that COMSOL can be used to predict gradient profiles in different designs and plot the result. It also proves that the second generation gradient generator is more versatile than the first generation gradient generator as it can generate a linear gradient profile. The flow profile in the culture chamber could also be simulated and plotted according to figure 28. Gradient generator PDMS stamps could be fabricated having channel widths of 200 μm and 100 μm if PVA treatment of the master was made prior to soft lithography. The culture chamber stamp was easily fabricated and would release from the injection mold if bubbles were not introduced during filling of uncured PDMS. Two PDMS stamps can be bonded together with a thin semipermeable membrane sandwiched in between. It is however very difficult to align the membrane and make it stick properly to the gradient generator stamp without trapping any air.

The questions stated in the hypothesis have been answered but there is much work that remains before a model system of the neural tube is constructed. Firstly, there is a need for more realistic 3D COMSOL simulations where the whole microfluidic device is modeled rather than the gradient generator and the culture chamber separately as they in reality are interconnected. Accurate values of the parameters used in the simulation should be found to obtain realistic simulations and evaluate the performance of the current microfluidic system. A value of the diffusion coefficient for GSK3i must for example be found and estimated for the used cell medium. Also a value of the viscosity of the cell medium is needed as it affects the value of the diffusion coefficient. Secondly, there are several changes that can be made to optimize the design of the microfluidic device and make it easier to operate. If a value of the diffusion coefficient and the viscosity is found it is possible to create a tailored microfluidic gradient generator having the necessary serpentine lengths and channel widths to assure that a linear gradient can be created. A major improvement in design which would simplify the device yet keep or improve the functionality is to instead of having vertical diffusion through the membrane, let the culture chamber flow be the same as the gradient generator flow. This change would result in a more robust system and would make it possible to reuse the microfluidic system many times as the semipermeable membrane is excluded. If this change was achieved it would mean that the medium consumption during experiments also would be reduced with 50% from a total of 320 μl/h to 160 μl/h as the gradient flow and the culture chamber flow is the same. There would be less inlets and outlets, as the new design would require three silicone tubings instead of eight, simplifying fabrication and experimental handling. Therefore only one pump would be needed for one device instead of three pumps. It would be easier to make COMSOL simulations as it is difficult to model diffusion through a semipermeable membrane without knowledge of porosity, diffusion in the membrane and thickness of the membrane. Thirdly, to model the neural tube it is necessary to create a microfluidic system capable of generating a 2D gradient. The first gradient with GSK3i mimics patterning along the rostro-caudal axis while the second gradient mimics patterning along the dorso-ventral axis. A future system will thus be more complex and perhaps require another flow based gradient generator to differentiate cells along the dorso-ventral axis.

8 Appendices

Appendix A - Master fabrication protocols

A1. Wet chromium etching

1. Develop mask by using a positive resist developer (Microposit 351), diluted 1:4 in Milli-Q-water, for 1 minute. Stir manually while developing. Positive resist patterned by the mask writer will be etched.
2. Wash mask in Milli-Q-water for 15 seconds and stir manually.
3. Dry mask properly using nitrogen gas.
4. Etch the mask with an undiluted chromium etchant (90 s).
5. Wash mask in Milli-Q-water for 1 minute and stir.
6. Dry mask again with nitrogen gas.
7. In case there are spots in the positive resist not patterned, put mask in acetone to remove all resist. Otherwise this step can be ignored.

A2. Spinning negative resist on glass wafer

1. Place a clean 4 inch glass wafer on a vacuum chuck in the spinner and start the vacuum pump to fix the wafer.
2. Apply 2 ml of negative resist (AZ 125-nXT-10A, AZ Electronic Materials) in the middle of the wafer with a Pasteur pipette. Try to avoid creating air bubbles in the resist.
3. Create a spin program with following parameters:
   (a) 1100 rpm / 4 s.
   (b) 550 rpm/ 30 s.

   This program should result in a resist thickness of 90-100 μm on the wafer.
4. Start the spinner.
5. If bubbles are seen on the surface of the resist, pop them using a sharp tweezer.
6. Soft bake the resist on a hot plate for 35 minutes with a temperature of 135 °C

A3. UV lithography

1. Attach the mask on the glass wafer with chromium side in direct contact with the resist.
2. Mount mask/wafer assembly in the mask aligner. No vacuum is necessary.
3. Configure exposure settings according to following recipe:

(a) Cycles: 7

(b) Shutter open: 60 s

(c) Shutter closed: 10 s

According to following recipe the resist is exposed to UV-light 7 times in 60 s intervals with a 10 s break between each interval.

4. Remove the mask/wafer assembly from the mask aligner. Lift off the mask from the wafer gently to avoid breaking the glass wafer. The mask pattern should now be transferred to the resist. A mask pattern can sometimes be seen in the resist before development.

A4. Development of negative resist

1. Place wafer in a negative resist developer (AZ 326 MIF Developer) using a wafer tweezer for 1 minute while stirring manually. The developer should change from transparent to a more orange color as all unexposed resist will dissolve in it.
2. Place wafer in Milli-Q-water and stir for 20-30 s to wash away dissolved resist from the wafer.
3. Repeat above steps 2 times or until the mask pattern is only seen on the glass wafer.
4. Wash wafer in new Milli-Q-water while stirring for 30 s.
5. Dry the wafer completely with nitrogen gas. A master is now fabricated.
6. Observe the master in a microscope to see whether all unexposed resist is dissolved. Otherwise, repeat steps 1, 2, 4 and 5 until only the mask pattern is seen on the master.

Appendix B - Soft lithography/ Injection mold protocols

B1. Preparation of PVA solution

Following protocol is for preparing PVA solution with a volume of 40 ml and a concentration of 0.125 (v/v)%

1. Withdraw 500 μl from an aqueous stock solution of PVA, 10 (v/v)% using a micropipette.
2. Add this volume into a 50 ml Falcon tube.
3. Add Milli-Q-water to get a total volume of 40 ml in the Falcon tube.
4. Mix solution properly by using a vortex.
5. Place the falcon tube in a dessicator and let the solution degas for 1.5 hours.

B2. PVA-coating of master

1. Place master in a plasma asher for 3 minutes to make the surface of the master hydrophilic.
2. Put master in a small container and add PVA solution, made according to protocol B1, until the top surface of the master is covered.
3. Lift up the master from the container by using a wafer tweezer. Then put it in a preheated oven (85 °C) for 5 minutes to evaporate the water.
4. Study the master under microscope to see whether the PVA coating has formed a rather thin and homogeneous layer. If not, it is possible to remove the PVA coating using MQ-water and repeat step 1-4.

B3. Preparation of PDMS

Following protocol creates a 1:10 mass-to-mass mixture (curing agent:base).

1. Add 25 g of Base from the Sylgard® 184 Silicone Elastomer Kit (Dow Corning) into a petri dish.
2. Add 2.5 g of curing agent, from the same kit, to the petri dish to get a 1:10 PDMS mixture.
3. Mix the two components properly using a plastic mixing spoon. An indicator is when small bubbles are formed throughout the entire mixture.

Appendix C Bonding protocols

C1. Spinning of thin PDMS glue on glass wafer

1. Mount a 4 inch glass wafer on a chuck with a diameter of 4 inches and start the vacuum pump to fix the wafer inside the spinner.
2. Deposit 1 ml of uncured PDMS in the center of the wafer. Avoid bubble formation in the PDMS. If bubbles are present on the surface, pop them using a sharp needle.
3. Create a spin program according to following protocol:
   (a) 150 rpm/ 30 s
   (b) 850 rpm/ 30 s
   (c) 2200 rpm/ 300 s
4. Put the lid on the spinner and start the spin program.
5. Release glass wafer from chuck by turning off the vacuum pump.

C2. Bonding of semipermeable membrane to gradient generator stamp

1. Observe gradient generator stamp under microscope to ensure all channels are clean from dust or other particles which could clog the channels after bonding. If dust is seen, use Milli-Q water to rinse the stamp and then dry with nitrogen gas.

2. Gently roll the PDMS stamp, with the channel structures pointing downwards, in the thin layer of uncured PDMS to avoid trapping air between the wafer and the stamp. Do not put pressure on the stamp to remove trapped air.

3. Release PDMS stamp from wafer. A thin layer of uncured PDMS serving as glue is now transferred to the contacted surface. **Warning: Make sure the stamp does not slide on the wafer when releasing the it; it could introduce uncured PDMS into the channels. Use two tweezers to avoid this.**

4. Place the stamp on a clean room wipe with the channel structures pointing upwards.

5. Attach a semipermeable membrane on the vertical channel region with two tweezers and ensure the membrane is completely in contact.

6. Similarly roll the culture chamber stamp in the thin layer of uncured PDMS, with the channel structure pointing upwards, to apply a thin layer of PDMS to the stamp. **Do not roll the stamp on the same place as the gradient generator stamp. Some surfaces might in this case not be coated with PDMS glue.**

7. Release the culture chamber stamp and contact it with the other stamp bonded to the semipermeable membrane. Make sure no air is trapped between the stamps. If air is trapped, pressure can be applied to remove some air.

References

[1] Hartung T. Hogberg H.T. Parmies, D. Biological and medical applications of a brain-on-a-chip. *Experimental Biology and Medicine*, 239:1096–1107, 2014.

[2] Huh D. Hamilton G. Ingber D.E. Kim, J.K. Human gut-on-a-chip inhabited by microbial flora that experiences intestinal peristalsis-like motions and flow. *Lab On A Chip*, 12:2165–2174, 2012.

[3] J.A Thomson. Embryonic stem cell lines derived from human blastocysts. *Science*, 282:1145–1147, 1998.

[4] Purves D. Augustie, G.J. *Neuroscience*. Sinauer, 2004.

[5] Krumlauf R. Lumsden, R. Patterning the vertebrate neuraxis. *Science*, 274:1109–1115, 1996.

[6] T.M. Jessell. Neuronal specification in the spinal cord: Inductive signals and transcriptional codes. *Nature*, 1:20–29, 2000.

[7] Jessell T.M. Edlund T. Nordstrom, U. Progressive induction of caudal neural character by graded wnt signaling. *Nature*, 5:525–532, 2002.

[8] J.L. Christian. Morphogen gradients: from form to function. *WIREs Dev Biol*, 1:3–15, 2012.

[9] Ericson J. Briscoe, J. Specification of neuronal fates in the ventral neural tube. *Neurobiology*, 11:43–49, 2001.

[10] Niswander L.A Liu, A. Bone morphogenetic protein signalling and vertebrate nervous system development. *Nature*, 6:945–954, 2005.

[11] A. Folch. *Introduction to BioMEMS*. CRC Press, 2013.

[12] H. Bruus. *Theoretical Microfluidics*. Oxford University Press, 2007.

[13] P.A. Davidson. *Turbulence: An Introduction for Scientists and Engineers*. Oxford University Press, 2004.

[14] Wereley S.T. Nguyen, N.T. *Fundamentals and applications of Microfluidics*. Artech house, 2006.

[15] Dertinger K.W. Whitesides G.M. Jeon, N.L. Generation of solution and surface gradients using microfluidic systems. *Langmuir*, 16:8311–8316, 2000.

[16] Jeon N.L. Whitesides G.M. Dertinger, K.W. Generation of gradients having complex shapes using microfluidic networks. *Anal. Chem.*, 73:1240–1246, 2001.

[17] Whitesides G.M.l Younan, X. Soft lithography. *Anal. Rev.Mater.Sci*, 28:153–184, 1998.

[18] Odom T.W. Chiu D.T. Whitesides G.M. Wu, H. Fabrication of complex three-dimensional microchannel systems in pdms. *JACS Articles*, 125:554–559, 2003.

[19] B.L. Welter. *Galaad 3 user manual.* 2005.

[20] Woodard J. Hansford D. Ferrell, N. Fabrication of polymer microstructures for mems: sacrificial layer micromolding and patterned substrate micromolding. *Biomedical Microdevices*, 9:815–821, 2007.

[21] Toh Y.C. Voldman J. Yu H. Kim, L. A practical guide to microfluidic perfusion culture of adherent mammalian cells. *Lab On A Chip*, 7:681–694, 2007.